REPUBLIC OF TÜRKİYE

ALTINBAŞ UNIVERSITY

Institute of Graduate Studies

Electrical and Computer Engineering

LADAR (LASER RADAR) DESIGN USING MICROSTRIP PATCH ANTENNA

Afnan Hamad SHIHAB

Master's Thesis

Supervisor

Assoc. Prof. Dr. Doğu Çağdaş ATİLLA

İstanbul, 2023

LADAR (LASER RADAR) DESIGN USING MICROSTRIP PATCH ANTENNA

Afnan Hamad SHIHAB

Electrical and Computer Engineering

Master's Thesis

ALTINBAŞ UNIVERSITY

2023

The thesis titled LADAR (LASER RADAR) DESIGN USING MICROSTRIP PATCH ANTENNA prepared by AFNAN HAMAD SHIHAB and submitted on 20/11/2023 has been **accepted unanimously** for the degree of Master of Science in Electrical and Computer Engineering.

Assoc. Prof. Dr. Doğu Çağdaş ATİLLA

Supervisor

Thesis Defense Committee Members:

Assoc. Prof. Dr. Doğu Çağdaş ATİLLA	Department of Electrical and Electronic Engineering, Altinbaş University	_____
Asst. Prof. Dr. Muhammad ILYAS	Department of Electronics and Communication Engineering, Altinbaş University	_____
Asst. Prof. Dr.Cahit KARAKUŞ	Department of Department of Computer Sciences and Engineering, Istanbul Esenyurt University	_____

I hereby declare that this thesis meets all format and submission requirements for a Master's thesis.

Submission date of the thesis to Institute of Graduate Studies: ___/___/___

I hereby declare that all information/data presented in this graduation project has been obtained in full accordance with academic rules and ethical conduct. I also declare all unoriginal materials and conclusions have been cited in the text and all references mentioned in the Reference List have been cited in the text, and vice versa as required by the abovementioned rules and conduct.

Afnan Hamad SHIHAB

Signature

ABSTRACT

LADAR (LASER RADAR) DESIGN USING MICROSTRIP PATCH ANTENNA

SHIHAB, Afnan Hamad
M.Sc., Electrical and Computer Engineering, Altınbaş University,

Supervisor: Assoc. Prof. Dr. Doğu Çağdaş ATİLLA

Date: 11/2023

Pages: 61

Multiple approaches have been explored to improve the data transfer rate and signal strength of this technology. Wireless communications in the 2.33 to 12.4 GHz range stand to benefit greatly from the new and enhanced square antenna proposed in this letter. With this antenna in place, new spectrums may be made available for wideband, license-free communications (UWB). In 2002, the United States Federal Communications Commission (FCC) officially recognized the ultra-wideband (UWB) frequency range of 3.1 GHz to 10.6 GHz.

The microstrip patch antenna, meanwhile, is often employed in high-frequency settings. In high-frequency settings, the microstrip patch antenna is a typical choice. The purpose of this thesis is to present a methodology for building antennas that make optimal use of the advantages of microstrip patch antennas in the context of ladar applications. The use of a THz rectangular microstrip patch antenna has been proposed. Polyimide, with a dielectric constant of 3.5, is our preferred choice for the substrate material. Therefore, the antenna's operating frequency will be between 0.648 THz to 0.68 THz. The computed resonance frequency of the proposed antenna is 0.8 THz, and its directional gain is 8.09 dBi. The antenna has a 30 GHz impedance bandwidth. At the resonance frequency of 0.625 THz, when the matching circuit is at its most effective, the modelled antenna's return loss was just -18.632 dB. The suggested antenna provides the flexibility to be used for a variety of applications, including Lidar, video rate imaging systems (0.6 THz), and homeland security (0.6–0.8 THz). CST Microwave Studio was used for both the antenna's design and its modelling.

Keywords: High Frequency, Ladar, Lidar, Microstrip Antenna, THz Applications.

TABLE OF CONTENTS

Pages

LIST OF TABLES

Pages

LIST OF FIGURES

Pages

ABBREVIATIONS

GPS	:	Global Positioning System
LaDAR	:	Laser Radar
NOAA	:	National Oceanic and Atmospheric Administration
GIS	:	Geographic Information Systems
MIC	:	Microwave Integrated Circuits
MMIC	:	Monolithic Microwave Circuits
UWB	:	Ultra-Wideband
OCT	:	Optical Coherence Tomography
GOI	:	Optics State Institute
FOI	:	Swedish Defense Research Establishment
ASEA	:	Allmänna Svenska Elektriska Aktiebolaget
NDRE	:	Norwegian Defense Research Establishment
RSRE	:	Royal Signals and Radar Establishment
ISAS	:	Information System Analysis and Synthesis
CTI	:	Coherent Technologies, Inc.
GMAPDS	:	Geiger-mode APD photon counting detectors

1. INTRODUCTION

The method of light detection and ranging is a type of remote sensing that measures distances on Earth by using a pulsed laser, hence the name of the method. Aerial systems have the capability of collecting other forms of data, such as laser pulses, in order to offer precise three-dimensional data on the shape and surface characteristics of the Earth.

The laser, the image scanner, and the high-precision GPS receiver are the major components that make up a ladar device. When collecting ladar data over a vast area, the most common vehicles used for data collection are airplanes and helicopters. This is because both of these types of vehicles can fly at a high altitude. It is possible to gather information using LaDAR in both a topographical and a bathymetric format. Bathymetric ladar makes use of a green laser that is able to penetrate water in order to detect the depths of the seabed and riverbeds. Topographic ladar, on the other hand, employs a near-infrared laser in order to scan the surface of the land.

Scientists and cartographers are able to evaluate natural and man-made environments with unprecedented precision, accuracy, and flexibility, according to the company, when they use Ladar technology. Researchers at NOAA are employing ladar for a number of objectives, including improving the quality of coastal maps, developing digital elevation models for use in geographic information systems (GIS), and aiding efforts to respond to emergencies.

On the market right now are very few portable scanning ladar devices that are safe for the eyes and have pulse energies that are high enough to allow for quick mapping of the environment in three dimensions. The number's first three digits in numerical order. In the process of design, achieving these attributes was one of the key aims that needed to be accomplished [1, 2, 3].

1.1 BACKGROUND

On the website known as Digital Coast [4], which is managed by the Office for Coastal Management, users will have access to the Ladar data sets for a wide variety of various coasts.

Laser radars are the only technology that can precisely measure the intensity of an item and create a picture of that object in three dimensions. Doppler lidar, the use of which has been gaining popularity recently, has the potential to offer information on the speed and vibration of an item. Such systems have a wide variety of applications, both in civilian and military settings, including terrain modelling, depth sounding, item recognition and classification, and object placement, to name a few. Researchers are also taking into consideration gated viewing, scanning lidars, 3D sensing focal plane arrays, and other types of scanners less lidar [5].

Even further, in 1997, [6] the United States Army Research Laboratory published a simulation method for determining the degree to which laser radar range estimates are inaccurate. After that, there was a significant uptick in interest in the imaging laser radar simulation technology. Both Boeing-SVS and the Swedish Defense Studies Institute provided work in the field of simulation to the research of algorithms for pulse signal processing [7].

In 2006 [8] [9] [10], Donoho, Candes, and Tao proposed what is now known as the compressed sensing hypothesis. Working with sparse or sparse expression signals does not preclude the possibility of properly recreating the original signal. This may be accomplished by reducing the measurement period and increasing the probability, respectively. In 2011, Holland from the University of Rochester achieved 3D compressed sensing imaging using photon counting in conjunction with a 780 nm pulse laser and a range resolution of 30 cm [11]. It was reported in 2016 [12] that Professor Sun of Beijing University of Aeronautics and Astronautics was able to produce 3D compressed sensing imaging with a resolution of 128 x 128 pixels and an accuracy of 3 millimetres at a distance of 5 meters by using a slicing approach and a pulsed laser. The research was carried out at a distance of 5 meters.

The performance of the laser three-dimensional imaging approach is dependent on a number of circumstances. These elements include the nature of the target and the environment in which it is located, as well as the level of complexity of the equipment that is used to analyse the reflected echo. As a result, it is essential to investigate and assess the methodology behind the signal processing.

As a result of the expanding imbalance between the country's energy demand and supply, which is prompted by the fast expansion of the economy, broad attempts are being made to construct new power plants. Without the ultrahigh voltage power transmission cables, it is not feasible to connect the national trunk network. The project to construct an ultrahigh voltage power transmission line is one of a kind in a variety of respects. The lengthy line distance, extensive region coverage, stringent security standards, mountain and valley crossings through dense forests, and significantly accelerated construction timeline are some of these benefits. When surveying ultrahigh voltage power transmission lines, there is a significant amount of physical labor needed, there is a high potential for making mistakes, and the process takes a significant amount of time. Using traditional surveying methods, it is not possible to ascertain either the height of the vegetation or the location of the electrical lines that traverse the region being surveyed.

1.2 PROBLEM STATEMENT

Essential to the development of laser radar technology, three-dimensional laser imaging has the capability of simultaneously collecting data on the target's geometric distribution as well as its reflection qualities. Its preeminence in the detection and identification of targets makes it applicable in a wide variety of military and civilian settings. Despite this fact, it is prohibitively expensive to do research and development on laser imaging equipment and technology. In order to create algorithms for signal processing and target recognition, a simulation model that is as precise as possible is required. The modeling and simulation of imaging laser radar is a worthy project given the great economic value of the technology as well as the vast number of potential applications it may have. When operating in the microwave frequency band, it is impractical to create conventional antennas. The smaller size of this antenna will make it possible to produce finished goods that are more compact. It is possible for the antennas to be simply etched onto any PCB over the course of the design and development process. This will ensure that they are easily accessible for troubleshooting purposes. This is possible due to the fact that the microstrip layout may be easily seen and accessible from the upper surface of the device. Because of this, they are easy to construct and may be used comfortably even on the curved surfaces of the gadget. As a direct

consequence of this, including these components into MIC and MMIC designs is a fairly straightforward process. When patch antennas are provided in an asymmetrical manner, there is a reduction in the amount of unwanted mode activation that occurs. Etching may be performed very simply on a variety of shapes, including rectangles, squares, and triangles. Because of the lower cost to generate them, they are more competitive for production in big quantities. They are efficient at a wide range of frequencies throughout the electromagnetic spectrum (dual, triple). Polarization can either be linear or circular, and one can be used in place of the other. They have a little amount of body fat. Because of the way that they are constructed, they have a very long lifespan when attached to a sturdy surface, such as the surface of a device.

Patch antennas, on the other hand, have a variety of limitations, such as a limited bandwidth and a low amplification factor. These shortcomings make patch antennas less desirable. Many different approaches have been tried in order to make this technology better in terms of both its bandwidth and its gain. This letter proposes the use of a new and improved square antenna with a frequency range of 2.33 to 12.4 GHz. If implemented, this antenna would make available greater bandwidth for unlicensed wideband communications (UWB). The ultra-wideband (UWB) frequency range, which spans from 3.1 GHz to 10.6 GHz, was given official recognition by the Federal Communications Commission (FCC) of the United States in the year 2002.

On the other hand, the microstrip patch antenna is often utilized for higher frequency applications.

1.3 OBJECTIVE

The microstrip patch antenna is often utilized for higher frequency applications. In the context of ladar applications, the objective of this thesis is to build antennas that are able to make full use of the benefits offered by microstrip patch antennas.

1.4 GENERAL OVERVIEW OF THE PROJECT

The fundamental components of a simulated laser radar imaging system are depicted in Figure 1.1 below. After being picked up by the detector, each individual laser pulse is converted into a single image pixel for the purpose of this simulation. To get the amplitude of the echo, you can use the pulse equation. After that, a number of different clutter processing techniques may be applied to the data in order to create range pictures with a variety of pixel densities.

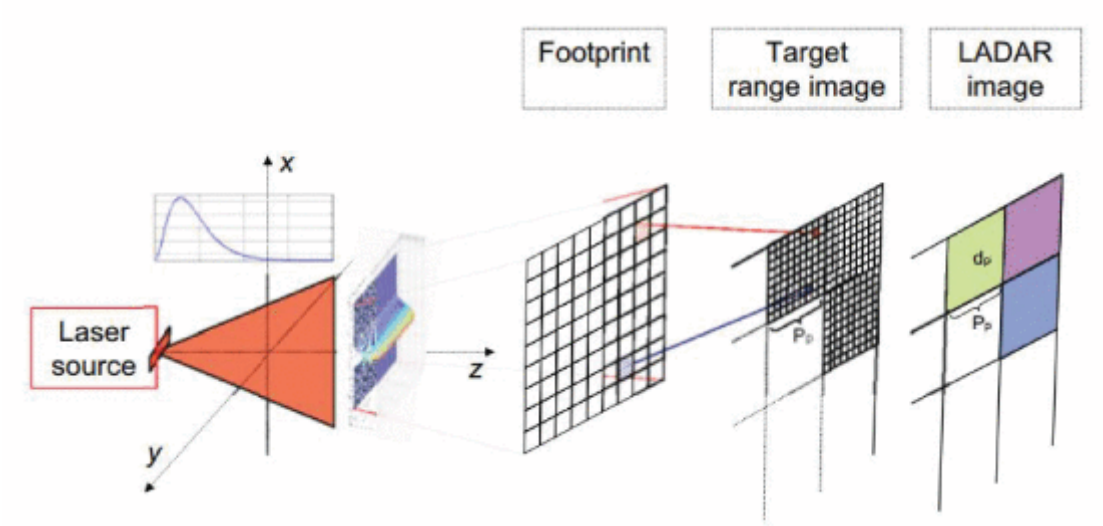

Figure 1.1: Conceptual Model.

1.5 THESIS OUTLINE

This thesis will be broken down into five major pieces. The introduction is the first chapter, and in it, a general explanation of the research's goals, problems, targets, and objectives is offered.

The second half of the thesis will be devoted to a review of the relevant prior work. This section offered background information on the potential applications of laser radar designs in order to achieve the objectives of the study.

In the next chapter, the approach will be explored in detail. In Chapter 3, we investigate whether or not the model may be utilized to achieve the goals that have been set.

The fourth chapter is comprised of the analysis and findings. In this part, we will present and analyse the results that were acquired.

The fifth and last chapter will provide the summary and end of the story. In this section, we covered the challenges that come with managing projects as well as the roles that each stakeholder plays in the process. It is planned to write a consensus as well as ideas.

2. LITERATURE REVIEW

2.1 LASER RADAR

In the early 1960s, not long after the laser was first introduced, development of laser radar (also known as ladar for laser detection and ranging, lidar for light detection and ranging, or opdar for optical detection and ranging) began in earnest. Other names for laser radar include: lidar for light detection and ranging, opdar for optical detection and ranging, and lidar for light detection and ranging. Work on lidar has been done in the past before the laser was created, but the laser has proven to be a wonderful enabler for this work. Laser radar is currently a competitive alternative to other sensor technologies such as passive electro-optical sensors and microwave radar as a result of its low cost, great reliability, and exceptionally rich phenomenology. These benefits make laser radar an attractive option. Laser radar first operated in the visible spectrum (using ruby lasers), then moved into the near infrared (using Nd:YAGlasers), and is now capable of operating in the thermal infrared as well (CO2 laser). Several different breakthroughs in laser radar are currently concentrating on short-wave infrared, which is measured in meters.

Along with the development of laser radar came a proliferation of scholarly works in the form of journals, conferences, symposia, and meetings. One example of this proliferation is the SPIE-organized "Laser Radar Technologies and Applications" session at the annual Defense and Commercial Sensing symposium, which provides attendees with dedicated laser radar training [13]. The topic of laser radar was covered in brand new introductory materials [14–17], research articles [18], and university courses [19]. Laser radar served as the conceptual foundation for the development of subsequent technologies such as optical coherence tomography (OCT) and digital holography. The majority of laser radar applications lie between a few micrometres [20] and tens of kilometres in range.

There are historical overviews of the development of laser radar available for Europe [21], the United States [22], the Former Soviet Union (FSU) [23], Japan [24], and China [25].

2.2 LASER RADARS AND DESIGNATORS WITH DIRECT DETECTION

The laser range finder is the kind of laser radar that is the most fundamental. To determine the distance between two points, a laser pulse is first sent at the target, and then the amount of time it takes for the pulse to return to the detector is measured. When we know the speed of light, we may calculate the distance between two points. Lebedev [26] was the first person to introduce the idea of determining a distance using light pulses of varied lengths. Because the pulses are so brief, it is feasible to get very high range resolution. In 1936, a particular interference modulator was developed for the purpose of being implemented in the prototype. At a distance of up to 3.5 kilometres, a precision of 2–3 meters was attained. In 1963 and 1964, the Vavilov Optics State Institute (GOI) in Leningrad constructed laser-based rangefinders made of ruby and gallium arsenide. This was done in the same facility that Lebedev had utilized in the 1930s (now St. Petersburg).

Late in the 1960s and early in the 1970s, the first military laser systems were created for use in range finders, proximity fuzzes, and missile guidance. These innovations were made possible by technological advancements in the laser industry. The first ruby lasers were extremely inefficient, costly, and some even caused permanent eye damage. Later on, Q-switched lasers brought about a revolution in the field of laser radar by enabling shorter pulses, greater energy, and more tightly collimated monochromatic beams.

Research on lasers was first carried out at the Swedish Defense Research Establishment (FOI) in 1961, and it was done using a ruby laser. ASEA and LM Ericsson were the first corporations to implement this strategy. The year 1968 saw Ericsson serving as a provider of laser rangefinders to the Swedish Coastal Artillery. Laser range finders were developed by Bofors in conjunction with Hughes Aircraft and installed in the IKV 91 infantry gun vehicle as well as the BOFI system. Following the conclusion of that time period, ASEA began developing cloud altimeters for usage in both the commercial and military sectors. When it was first released in the early 1970s, the anti-aircraft missile beam rider system known as the RBS 70 by Bofors was an instant hit all over the world. Bofors is credited with developing the world's first laser beam rider surface-to-air missile that was capable of actual combat. In the late 1970s, Ericsson was responsible for developing the laser-based proximity

fuses that were used in the Sidewinder missile. Despite the fact that Ericsson developed a laser tracking system, this technology was rapidly rendered obsolete by video trackers.

Portable binoculars equipped with a laser range finder have been developed by Simrad Optronics with assistance from the Norwegian Defense Research Establishment (NDRE). In more recent years, the company has developed a variety of range finders that may be used for locating specific targets and controlling the rate of shooting.

The Royal Signals and Radar Establishment (RSRE) of the United Kingdom was an early adopter of military laser technology. Forrester and Hulme [27] provided a detailed account of the early advancements of laser range finders. It is believed that the LF-2 ruby tank laser sight was the first laser system to be manufactured in big quantities anywhere in the globe. However, the cannon was finally placed on the Vickers MBT, Centurion, Scorpion, and Chieftain derivatives. The Chieftain main battle tank used by the British army served as the inspiration for its design. The old equipment was a ruby laser with a revolving prism Q-switch, but it has since been replaced by a YAG laser that is passively Q-switched (LF-11).

In 1968, Ferranti, which is now known as Leonardo Finmeccanica, introduced the world's first entirely stabilized laser system by including a Nd:YAG laser range finder and marking target seeker into the device. This innovation significantly changed the industry. The airplane is equipped with something called a marking target seeker, which allows it to focus in on a target that has been marked with a laser and then follow it. The weapon targeting systems of the Jaguar, Harrier, and Tornado aircraft were all outfitted with similar pieces of equipment. The power for the 1.06-m laser transmitter came from an electro-optic Q-switched Nd:YAG laser, which can operate at either 10 or 20 Hz repetition rate.

In a subsequent publication published by SPIE [28], information regarding an early Soviet laser rangefinder known as the BD-1 (Figure 2.1) was provided. A further illustration of this is the KTD 2-2. In more recent writing [29], a broad variety of operational devices that make use of laser technology are described. Some examples of these devices are laser range finders and laser designators. Both fixed- and rotary-wing aircraft, such as the SU and the MIG, as well as airplanes such as the SU and the MIG can be equipped with them (see Figure 2.2). 1967 saw the delivery of a Nd:YAG laser range finder by Thales Research and Technology

to a number of French government entities. In order to conduct tests more effectively, the AMX 13 tank was modified with a laser rangefinder [30]. In the 1970s, Thomson and Cilas developed an airborne target illumination system that served as a forerunner to the ATLIS targeting pod and demonstrated the capability of being mounted on a single-seat jet fighter.

In Germany, Carl Zeiss and Eltro developed laser range finders and target designators by employing the Nd:YAG laser as their primary source of light. Research on lasers was carried out for the military by FGAN-FfO. Many of their early research [31] focused on the propagation of laser light through the atmosphere.

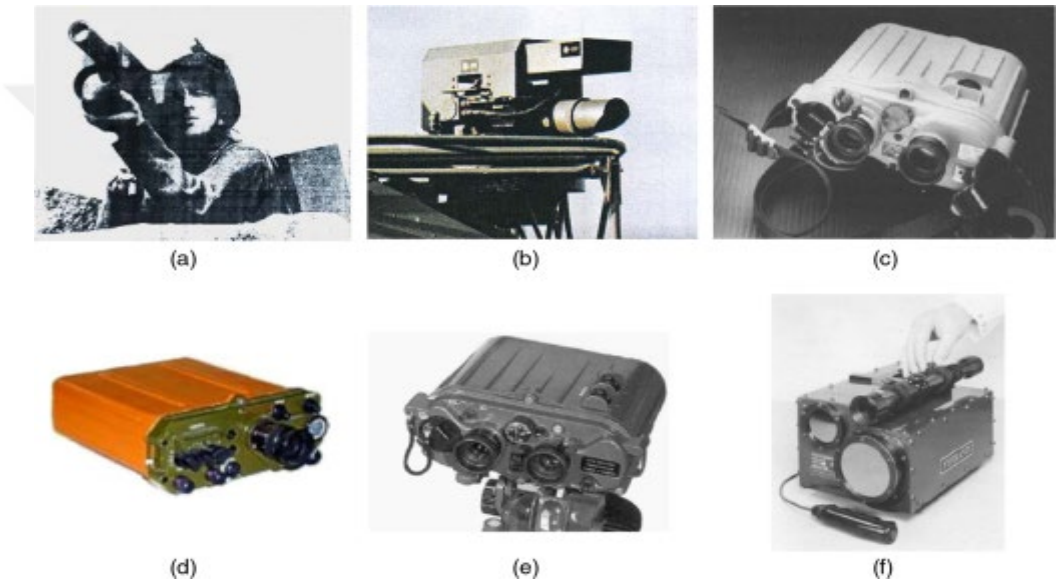

Figure 2.1: Predecessors of Current Laser Rangefinders (LRFs). From Left to Right: (a) Ericsson's Initial LRF Testing Equipment From 1965; (b) an LRF Used by The Swedish Coastal Artillery in 1968; (c) a Portable LP-7 From Simrad; (d) a Polyus LRF; (e) a BD-1 From The INSTITUTE #801 in The USSR; and (f) a Ferranti CO2 TEA LRF. Ericsson was One of The First Companies to Develop Equipment for Testing LRF.

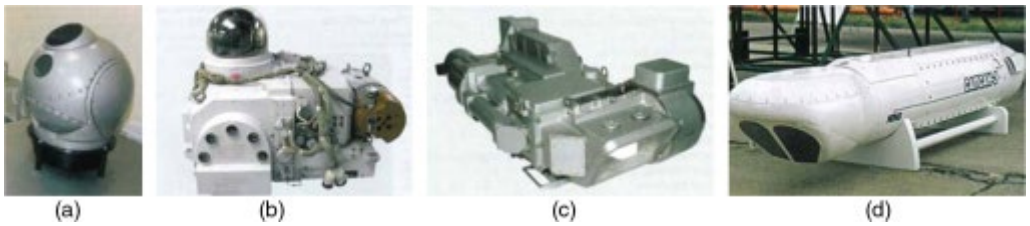

Figure 2.2: Russian and Soviet Examples of Laser Range Finders and Designators.

2.3 LASER-BASED SYSTEM COMPONENTS, INCLUDING RANGEFINDERS AND DESIGNERS

After the development of ruby and Nd:YAG laser range finders and target designators, concerns emerged regarding eye safety and range finder compatibility with FLIR in the 8 to 12 m zone. It was necessary for the rangefinder to be able to see through smoke and mist to any target that could be identified by the thermal imager. The development of pulsed range finders required the use of the pulsed CO2 TEA laser because of this reason. This CO2 TEA prototype functions as a rangefinder and was developed jointly by RSRE and Ferranti [32]. Unfortunately, the CO2 TEA range finder was not successful. The "wet target problem," in which range is lost from wet targets because of low reflectivity at 10.6 m, the requirement for cooled detectors, the high cost of optics, and concerns regarding the laser's lifetime all contributed to the fact that only a small portion of these systems were ever put into service. Soon after that, the major emphasis of military laser range finding was switched from 1.06 to 1.55 m using a Raman-shifted optical parameter oscillator or high-pressure gas technology. This modification occurred not long after. Alternate designs called for the utilization of erbium glass or other types of materials. The utilization of an effective Nd:YAG laser as a pump source gave rise to the concept of multifunctional lasers [33]. The idea was to incorporate a number of functions, such as laser radar and laser jamming, as well as "friend or foe" identification on the battlefield, into a single, compact device that would be centered on a single transmitter that would operate at 1.06 - m. The plan called for the device to be as small as possible. In Figure 2.3, there are several instances of systems from the time of the Soviet Union that make use of laser rangefinders and designators.

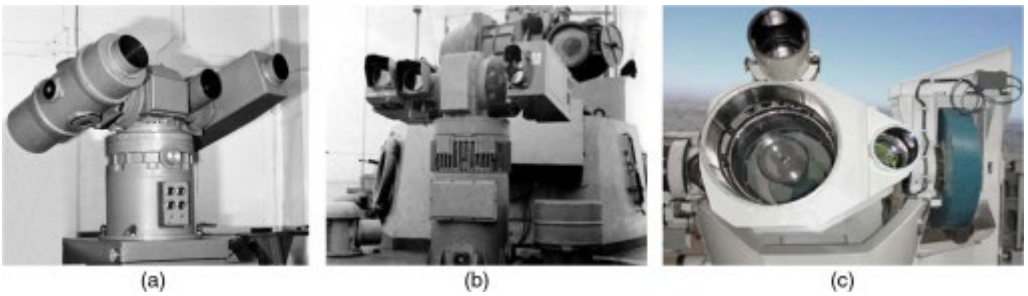

Figure 2.3: EOS-LR (Laser-Radar) Systems Deployed by The FSU.

2.4 LASER ALTIMETERS

Time-of-flight measurement is one of the most important aspects of laser radar altimeters. The Lunar Orbiter Laser Altimeter, or LOLA, was created by the National Aeronautics and Space Administration (NASA) of the United States of America in order to precisely map the surface of the Moon and investigate possible landing sites. The basic measure that is used in LOLA is a surface's topography. Additionally, the device is able to measure the reflectance, roughness, and slope of the surface. LOLA is a multibeam laser altimeter that operates with a pulse repetition rate of 28 Hz and a wavelength of 1064.4 nanometres. A single laser beam is split into five output beams by a diffractive optical element in order to achieve a sampling rate of 140 measurements per second (Figure 2.4(a)). Each of these five output beams has a 100-mrad divergence and lights a 5-m diameter spot from the mapping orbit. This allows for a sampling rate of 140 measurements per second. The receiver is able to detect the pulses that were backscattered because it projects the five-spot pattern onto individual optical fibres. These optical fibres then pass the signal on to individual silicon avalanche photodiode (APD) detectors so that the receiver can pick up on the pulses. Figure 2.4 displays an example of a lunar profile (b).

The laser beams make a cross-shaped intersection with the surface of the moon at an angle of 500 milliradians (mrad) and 26 degrees of rotation about the nadir axis with respect to the spacecraft's forward velocity vector. Because of the way the samples are designed, it is possible to assess the slope of the surface from a variety of angles. Figure 2.4 illustrates a lunar topographical map (c).

Inoue et al. [34] from Toyota used fibre amplifiers for both transmission and reception to increase the sensitivity of laser radar for use in automotive applications. The sensor head used in this research had a surface area of just 2 cm 2 (square centimetres). In order for the transmission optical system to function properly, it relies on a pulsed fibre laser. The pulse is four nanoseconds wide, and the maximum output power is ten kilowatts. The diameter of the scanning mirror is 10 millimetres. The optical fibre amplifier has a mid-way isolator and a band-pass filter built into it to cut down on the amount of spontaneous emission, increase

conversion efficiency, and minimize the amount of noise figure [35]. A resonance frequency of 100 Hz is achieved by the scanning mirror, which also has a scanning angle of 40 degrees.

The ISAS institution of the Japanese government is responsible for the development of the several laser altimeters that are utilized in astronomy and space research. The mission of the Hayabusa lidar, which began in 2005, is broken down into its component parts and presented in Figure 2.5. 26,27 Figure 2.5 depicts a flight model of the ISAS, and Figure 2.5 also depicts an imager taking a picture of the asteroid Itokawa (size: 540 m 270 m 210 m). It weighs 3.7 kilograms and measures 24 by 23 by 25 centimetres, and its effective wavelength is 1064 nanometres. Its output is 8 millijoules at one hertz through an aperture of 12.5 centimetres. The relative height as measured by the Hayabusa laser radar is depicted in figure 2.5. It is possible to reach a range resolution of 1 meter. To the best of our knowledge, this is the very first accurate measurement of the height of an asteroid. With the help of the Hayabusa-2 laser radar, researchers from around the world attempted in 2015 to bring the asteroid 1999 Ju3 within range of Earth.

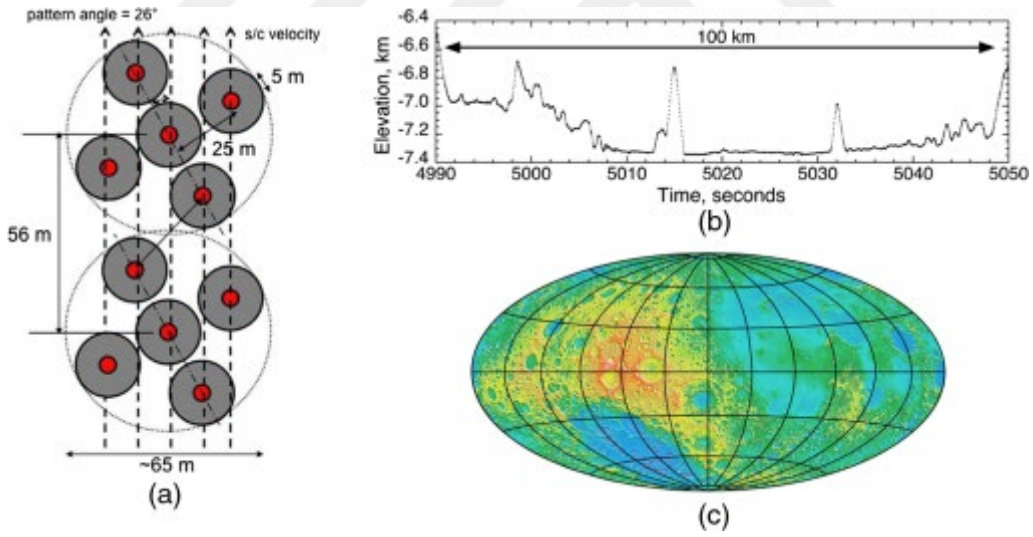

Figure 2.4: Five Laser Beams From The Lunar Orbiter Laser Altimeter (a), Lunar Profiles (b), and a Topography Map of The Moon (c).

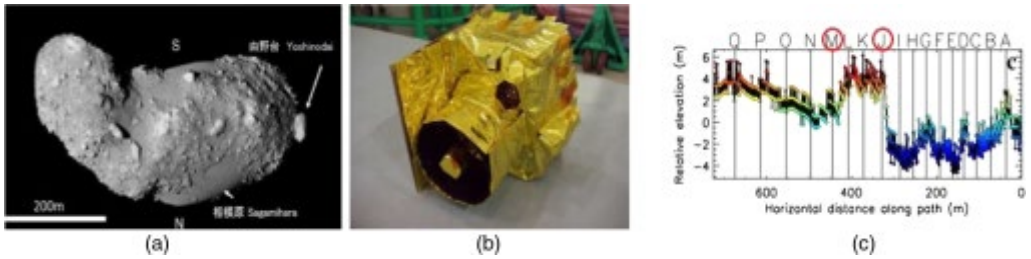

Figure 2.5: A Lidar on Board The "Hayabusa" Spacecraft.

2.5 NONCOHERENT WIND MEASUREMENT

In a demonstration of the capability of a noncoherent laser rangefinder to calculate wind profiles at low altitudes, small and lightweight balloons with a diameter of 0.25 meters were employed as the test subjects [36]. Laser range detection (0.5 m) in combination with azimuth and elevation measurements offers an easy, accurate, and cost-effective alternative to standard wind profiling approaches, as shown by the results of studies employing balloon trajectories. In order to increase the maximum detection range to 2200 meters, retroreflector tape was affixed to balloons and used in their construction. LEDs with low power requirements made it feasible to maintain visibility of items even when they were in the dark (LEDs).

Another instance of noncoherent Doppler wind measurement may be found in the article that was written by Liu and his colleagues [37]. Ocean University in Qingdao, China, is where Liu received his education, and his colleagues at NASA Langley Research Center in Hampton, Virginia, are regarded as some of the most talented in the field. A diagram illustrating the transmitter, receiver, and frequency control of the lidar may be seen in figure 2.6. Two diodes are used to pump the Nd:YAGseed laser, which is a single-mode oscillator that has the ability to have its wavelength altered. A Continuum Powerlite 7000 Nd:YAG pulsed laser receives output at 1064 nm, which is then pumped into it. For the purpose of controlling and locking the seed laser frequency, the output of the laser at 532 nm must be sent via an iodine filter (cell 1). We are able to keep the frequency accurate to within 0.2 MHz when utilizing this arrangement, which is comparable to an uncertainty in wind speed measurement of 5.0 cm/s.

Using a transportable direct-detection Rayleigh-scatter Doppler lidar (Figure 2.7), the University of Science and Technology of China [38] was able to measure wind fields from a distance of 15 to 70 kilometres, with a height resolution of 0.2 kilometres below 40 kilometres and 1 kilometres above. This no scanning system makes use of a frequency tripled 50 Hz Nd:YAG laser to create a wavelength of 354.7 nm. This wavelength is safe for usage in close proximity to the eyes and may be used for a variety of applications. Employing a triple channel as a frequency discriminator, the wind velocity may be determined by using two double-edge channels that are placed in the wings of the thermally widened molecular backscattered signal spectrum [39]. The third channel uses the intersection of the double-edge channels as the point at which it locks the frequency of the outgoing laser. The emitting-receiving system is scanned in a continuous manner by the scanning system, which enables the scanning system to detect the horizontal wind from all four cardinal directions (north, south, east, and west).

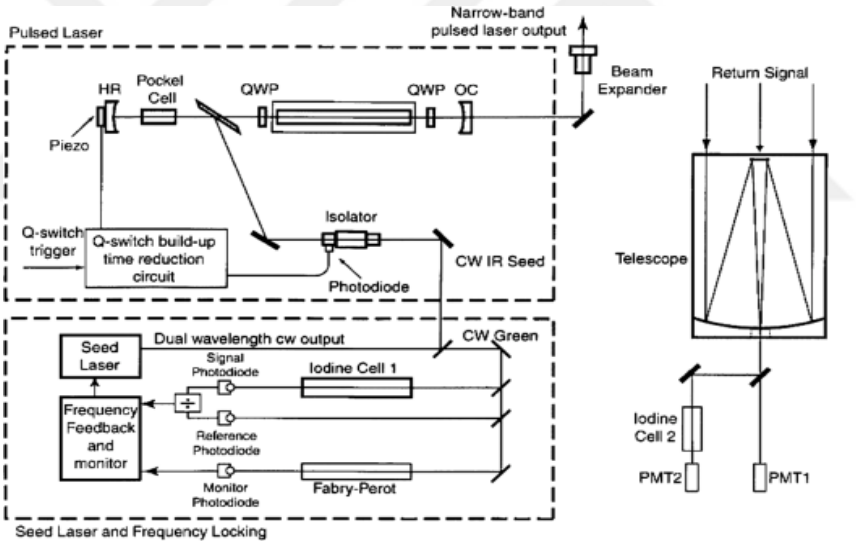

Figure 2.6: Schematic of a Q-Switched, Pulsed Nd:YAG Laser Transmitter with Injection Seeding.

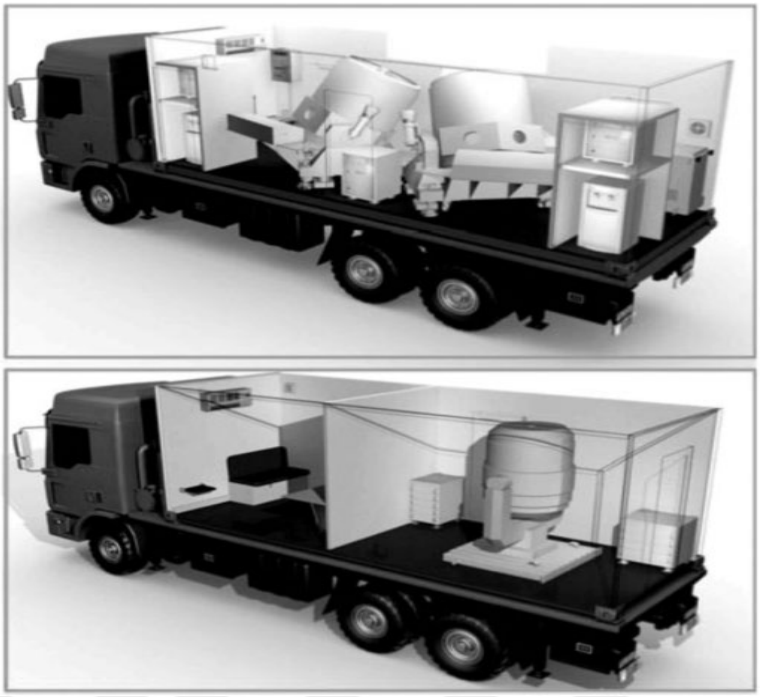

Figure 2.7: Dual-Lidar Perspective.

2.6 COHERENT LASER RADARS

2.6.1 Vibrometry

A prospective use for coherent laser radar is vibrometry, which makes advantage of the Doppler effect. Readings taken from a distance and without direct touch might be useful for a wide range of equipment, both civilian and military. Vibrometers typically operate at a frequency of either 1.5, 2, or 10.6 m on average. In order to get vibrational data that is spatially resolved, scanning and multibeam laser vibrometers are employed. Target classification and identification, including targets that are camouflaged or partially concealed, as well as the detection of buried land mines are just a few examples of the defence and security applications that are highlighted in reference [40]. However, there are also some examples of civil medium-range applications. The resulting vibration spectrum is an essential and trustworthy component that may be used when attempting to categorize or identify a target. The minuscule target that is depicted in Figure 2.8 is a typical black rubber boat that is propelled by an outboard engine. The boat has a total capacity of 422 m3 of space. The range was much less than one kilometre. The frequency spectrum is represented

in the graphic in the centre of the page. The vibrations originate from a wide variety of locations throughout the item. On the right you can see the 5-s spectrogram that corresponds to the signal.

A coherent CO2 laser was used to extract vibration signatures from the LACE satellite using a method that was based on a spectrogram while laser radar measurements were being taken from the ground [41]. The satellite was supplied with IR germanium retroreflectors on deployable/retractable booms so that ground-based IR laser radar measurements of on-orbit boom vibrations may be improved. The data was gathered both in the course of and immediately following one of the surgeries (boom retraction). They provided evidence that indicated to the presence of a complex mode structure that altered and developed throughout the course of time. The Doppler-time-intensity method in which vibrational power spectra are shown may be seen in Figure 2.9. The vertical axis of time here corresponds to the power spectrum. Doppler frequency, shown along the vertical axis (i.e., velocity).

In addition to CO2 lasers operating at a wavelength of 10.6 meters, a number of solid-state laser sources based on neodymium at 1.06 meters, semiconductors or erbium fibre at 1.5 meters, and holmium at 2.1 meters have been utilized in the construction of laser vibrometers. However, there are circumstances in which it may be beneficial to run in the mid-IR range in order to increase system performance. One example of this is when visibility is limited, winds are strong, or humidity levels are high. Running in this band can help. These kinds of conditions are rather common in places like low-lying areas and near the seashore. When compared to shorter- or longer-wavelength systems, mid-IR coherent laser radar systems' resilience to scattering, turbulence, and humidity may be beneficial in low-altitude situations. These conditions may also benefit from the systems' ability to detect targets more precisely. The research paper referred to above (Ref. 42) describes the development of a monostatic coherent laser radar at 3.6 m, which made use of an optical parametric oscillator with a single frequency [42]. It worked outdoors across relatively short distances and utilized two parked cars with running engines as targets. The measurements from the system's micro-Doppler could be used to compute the surface vibration spectra of the automobiles while they were idling.

Obtaining a spatial distribution of vibrations on the surface of the object being investigated may be accomplished through the use of a scanning vibrometer. Using a scanning laser vibrometer can cut down on the amount of time needed for testing if a large number of measurement points are required. This type of vibrometer enables examination of the structure with high spatial resolution without affecting the structure's dynamic behaviour. In order to investigate the problem of taking measurements while in flight, vibrations were examined by employing a scanning laser Doppler vibrometer inside of a cabin mock-up of an Agusta A109MKII. The overall viewable area has a dimension of 430 millimetres squared. In order to conduct the scanning tests, a 30 by 20 grid was used. In addition, vibration records made with the instrument when it was not attached to the model were compared. Figure 2.10 provides a summary of the findings of the resonance tests. The bandwidth is ten hertz (Hz) for frequencies up to one thousand hertz, and it is thirty hertz (Hz) for frequencies up to five thousand hertz. The instantaneous amplitude of the velocity component orthogonal to the surface is used to describe each of these variables. In addition to that, research was done to determine whether or not it would be possible to use vibration sensing to find underground mines [43].

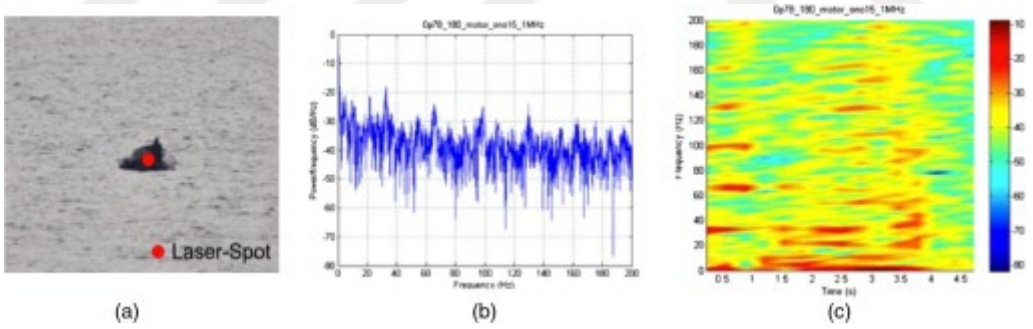

Figure 2.8: Rubber Boat Vibration Analysis.

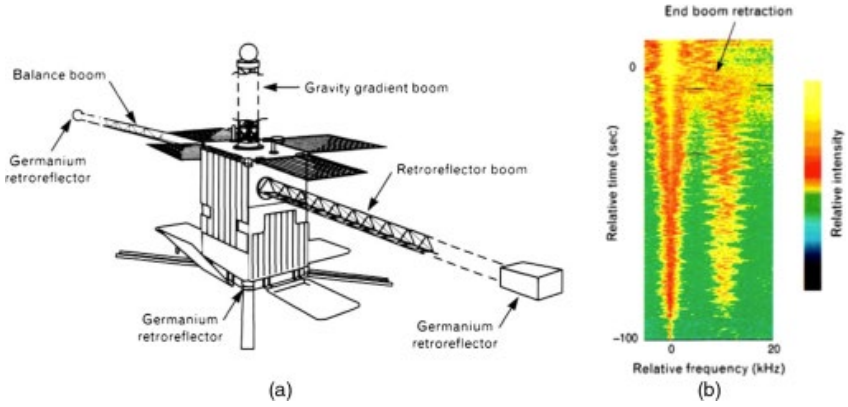

Figure 2.9: LACE Satellite.

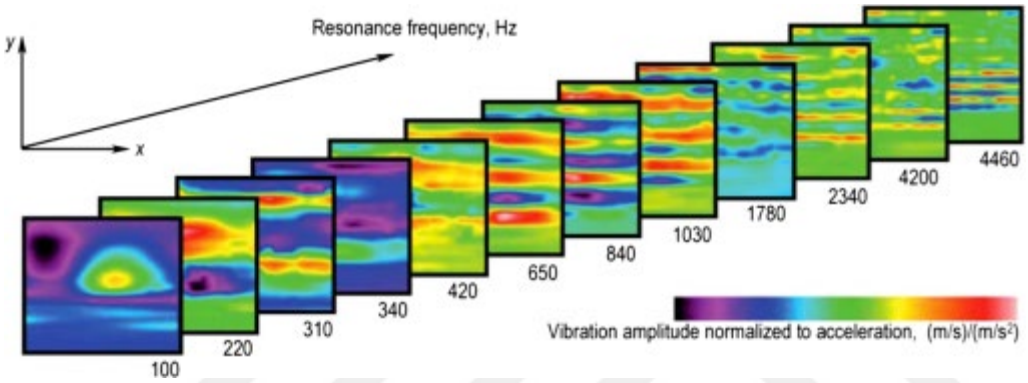

Figure 2.10: A Number of Resonance Vibration Frequencies Were Detected Within The Helicopter Replica's Cockpit.

2.6.2 Atmospheric Wind Sensing

Wind sensing is one application that can benefit from using coherent laser radars [44]. In addition to these local wind field measurements and wake vortex research at airfields, a number of additional ground-based efforts are utilized in order to obtain the data (Figure 2.11). The real airspeed, pressure error, wind shear warning, and atmospheric backscattering are evaluated by airborne instruments when flying across the North and South Atlantic. During the 1990s, the European Space Agency provided money for a program called the Atmospheric Laser Doppler Instrument, which was responsible for the development of a satellite-based wind lidar. Research on wind lidar was pioneered in Europe by RSRE (located in the United Kingdom), DLR (located in Germany), and the Laboratories de Meteorology Dynamique, located at Ecole Polytechnique (France). This paper by Vaughan

et al. offers a detailed review of the initial efforts made to develop a coherent laser radar in Europe. 40 Early coherent laser radars in the United States are the subject of extensive coverage in the edited volume [45] compiled and edited by Killinger and Mooradian.

It would appear that coherent Doppler lidar, also known as CDL, may be an extremely helpful instrument for detecting winds in the atmosphere, whether done so from the ground, the air, or space. The high spatial and temporal resolution at which CDLs survey large portions of the atmosphere makes the data they collect relevant for a wide variety of applications. This is due to the fact that the data may be put to use in a number of different ways.

In 1970, Huffaker et al. [46] first utilized a continuous-wave CO2 laser at a distance of 10.6 meters in order to identify wake vortices. After developing a high power fiber amplifier of Er, Yb:glass with 3.3 kW output power, 580 ns width, and 4 kHz repetition rate [47], Mitsubishi Electric started selling eye-safe small fiber-based lidars and middle-range (8 km) wind lidars in the late 1990s. These lidars were able to measure wind speeds up to 8 kilometers away (Figure 2.12). This amplifier was also utilized to produce a wind lidar with a range resolution of 300 m, which is ultra-long range and exceeds 30 kilometers [48]. This amplifier was employed. An all-fiber CDL was also developed on the basis of this innovative notion, which entails automatic parameter control that is responsive to atmospheric situation. These instruments have a wide variety of applications in industry, including but not limited to meteorological monitoring, wind surveying for wind power generation, aviation safety, and many more.

In the 1990s and early 2000s, Coherent Technologies, Inc. (CTI), which received support from both the Air Force and NASA, was the driving force behind the development of wind sensing technology. CTI was responsible for the industrial production of a variety of goods, including the Wind Tracer. A great number of Wind Tracer systems have been installed at airports as well as universities in order to monitor wind shear in the vicinity of airports and research airplane wake vortices.

Tracking the wind speeds in wind farms has also made use of a technology quite similar to this in more recent times. These sensors are mounted on the top of the tower to monitor the

flow of air and the level of turbulence. This helps to ensure that the wind turbines are operating as effectively as possible. In the United Kingdom, you may acquire these items from Halo Photonics, while in France, you can get them via Leosphere.

For use in air drop, gun ship, and dumb bomb operations, the United States Air Force is very interested in developing wind-sensing technologies. The airborne version of ballistic winds was evaluated with the use of a nearly prototype C-130 Pod System. The monster weighed 1000 pounds and had a volume of 15 cubic feet. We made use of a solid-state laser with a wavelength of 2 meters and an output energy of 15 mJ.

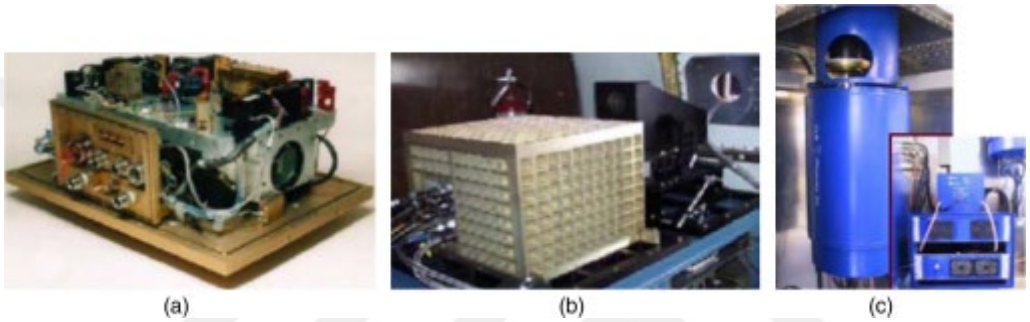

Figure 2.11: Wind Sensors.

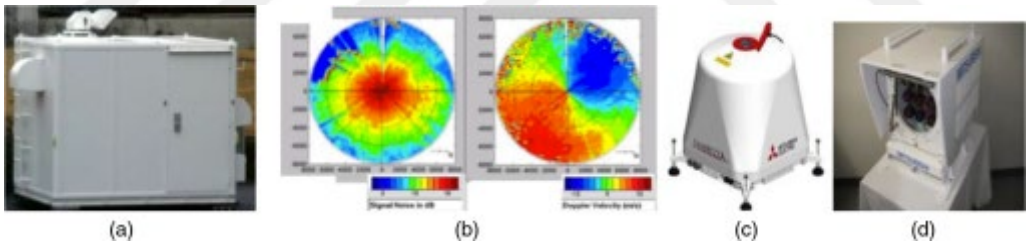

Figure 2.12: CDL.

2.6.3 Airborne Applications

Coherent laser radars make use of the spatial and temporal coherence of laser light in their operation. In direct detection, the strength (amplitude) of the return laser signal is all that is measured. However, the entire field can be evaluated by mixing the received signal with an optical local oscillator, which provides information about both the phase and amplitude of the field. This is in contrast to direct detection, which only measures the strength of the return laser signal. Since the Doppler frequency shift can be estimated directly from the recorded

phase, coherent laser radar is frequently used for measuring velocity. This is one of the most prevalent use cases for this type of radar.

Airborne coherent laser radars make it feasible to perform a wide variety of sensing and imaging functions, including ground imaging, obstacle warning, terrain tracking, and wind sensing (including backscatter measurements). A method known as CLARA was developed in France and the United Kingdom for the purpose of taking measurements of hard objects (cables, ground surface, etc.) [49]. The construction of this gear was spurred by the successful testing of a pulsed CO2 laser radar known as the "laser obstacle and cable unmasking system." This radar was created by two divisions of the formerly known company GEC Marconi. Another research [50] conducted in France by the Société française d'équipements pour la navigation aérienne demonstrated the use of a frequency-modulated continuous-wave (FMCW) laser radar for terrain following and terrain avoidance by combat aircraft. The RSRE-developed LATAS airborne lidar [51] was able to exhibit intensity imaging of both natural terrain and man-made objects; nevertheless, its primary objective was to measure real air speed and atmospheric backscatter at a distance of 10.6 meters.

Applications like as rendezvous and docking with orbiting spacecraft, as well as precise navigation to a designated landing location on Earth or on alien objects, require accurate information on the relative velocity and altitude of the vehicle. This information is important for the application. The ALHAT project [52] of NASA culminated in the invention of a Doppler lidar, which supplied the navigation system with accurate vector velocity data that it utilized to follow the vehicle's movement toward the landing place in real time.

Figure 2.13 depicts the assembly of an all-fiber lidar in its finished state. A frequency-modulated waveform is generated by a fiber laser with a narrow linewidth, and it is then sent over a single-mode fiber to an amplifier, which increases the intensity of the signal. From the output of the fiber amplifier, power is distributed to three optical channels; one channel is designated for each of the vector components of velocity (Figure 2.14).

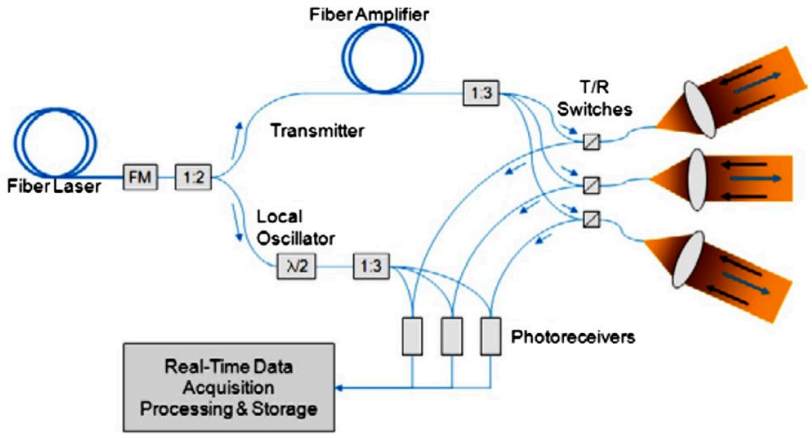

Figure 2.13: Setup of a Doppler Lidar System.

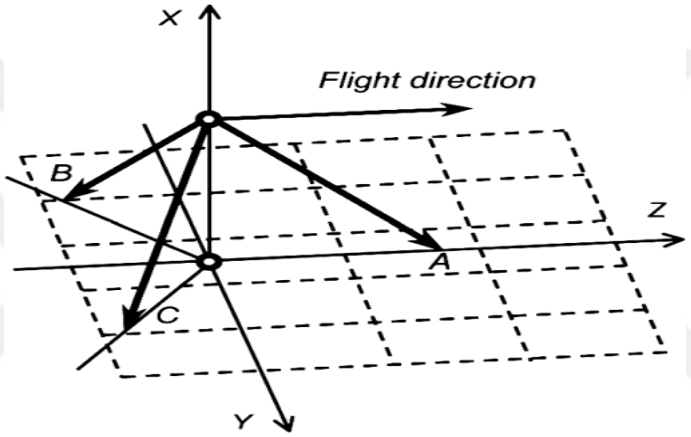

Figure 2.14: Sensor Geometry Expressed as a Set of Unit Vectors.

2.7 ENVIRONMENTAL LASER RADARS (LIDARS)

After first concentrating their efforts on laser sensing for the military, researchers in the field of laser radar eventually expanded their work to encompass sensing for the atmosphere and the ocean. For instance, Fiocco and Smullin [53] conducted laser radar research on the mesosphere using a ruby laser in the year 1963. The dispersion of aerosols across the troposphere was reported by Collis et al. [54] The first experiment using differential absorption lidar was carried out in the United States in the year 1960. It entailed the investigation of vertical water vapor dispersion using a temperature-tuned ruby laser. The experiment was carried out in the year 1960. (DIAL). The Japanese were the first people to build an Mie scattering laser radar by using a Q-switched ruby laser that they had made themselves at home. In a study conducted in 1968 at Tohoku University by Inaba et al. [55],

the researchers looked at basic links between scattering, extinction, and visibility. Arshinov et al. [56] looked into the temperature of the atmosphere in the FSU and found some interesting results. In the course of their study, Zuev and colleagues [57] investigated whether or not it would be possible to make use of lasers to measure the vertical profile of atmospheric humidity. Figure 2.15 is a representation of the many different kinds of lidar systems [58]. The first Chinese atmospheric laser radar reportedly went into service in the year 1965, as stated by Hu and Qiu66. Since that time, scientists have carried out a variety of experiments in order to gain a deeper understanding of the ozone profile in the stratosphere, the density of volcanic clouds, the extinction coefficient of aerosols, the intensity of atmospheric turbulence, the sodium layer and Rayleigh scattering in the middle atmosphere, the temperature of the ocean and the presence of oil slicks on its surface, and a great number of other factors. In addition to this, a substantial amount of theoretical investigation was carried out. Svanberg details numerous pioneering use of laser radar in the field of pollution monitoring. Both atmospheric and oceanic laser radars can employ a broad range of lasers and detectors, depending on the use for which they were designed. Sensing of aerosols or gases, sensing of the ocean (including bottom profiling or water sensing), and ocean sensing are all examples of possible endpoints (turbidity, plankton, and so on). Within the confines of this study, there is insufficient space to go into further depth about the development of air and ocean lidar. Instead of looking at this, the reader should consult the textbooks and the reviews [58]. The passage of laser light through a medium consisting of water is investigated in two other papers [59]. In the former Soviet Union, Tatarskiy [60] and Zuev [61] conducted research utilizing environmental laser radars, and based on their findings, they authored influential monographs on the atmospheric propagation of laser radiation. After that, other monographs emanating from the Tomsk school of science were published [62]. This book was developed specifically for meteorologists, and its primary focus is on the various practical challenges that have surfaced as a direct result of the application of meteorological principles [63]. Agishev [64] discusses the developments that have been achieved in CW FM technology in his article.

Penn State University has made significant strides in the field of Raman laser radar [65], which is an acronym for that field. They made it possible to measure the optical and

meteorological properties of the atmosphere based on the vibrational and rotational energy states of molecular species like water vapor and ozone, as well as temperature, optical extinction, optical backscatter, multiwavelength extinction, extinction/backscatter ratio, aerosol layers, and cloud formation/dissipation. These measurements were based on the vibrational and rotational energy states of molecular species like water vapor and ozone (Figure 2.16). Measurements of the scattering phase function for aerosols, such as the polarization ratio of the scattering phase function, number density versus size, size distribution, identification of multicomponent aerosols, index of refraction, and so on, significantly improve the quality of the information that is obtained through an angular scattering technique. Possible avenues of investigation include multiwavelength multistate laser radar and multistate aerosol laser radar.

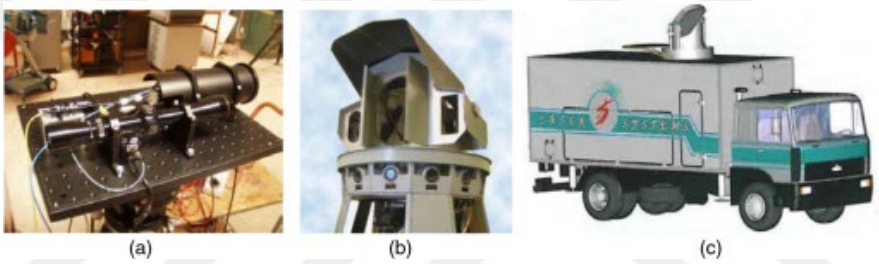

Figure 2.15: Lidars for Atmosphere Investigation.

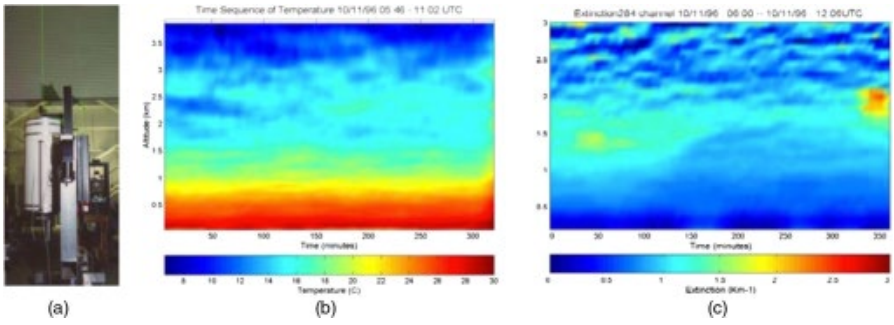

Figure 2.16: Lidar at The Pennsylvania State University.

2.8 3-D LASER RADARS

The invention of three-dimensional flash laser radars, which offer information on intensity and range in each pixel from a single illuminating pulse, was a driving force behind the investigation of focal plane array detectors. Due to the high level of interest in HdCdTe-

based APD arrays and the potential benefits they may provide, a number of firms, including Raytheon, DRS, Sofradir/Leti, and Selex, are now working on developing these arrays. A significant amount of money is spent on research and development not just for linear APD arrays but also for Geiger-mode APD photon counting detectors (GMAPDs). MIT/LL has been in the forefront of developing GMAPDs for use in innovative laser radar systems like Jigsaw. These GMAPDs have been used in a variety of projects. The capacity of jigsaw 3-D laser radars to "poke through" obstructions like as camouflage and vegetation is one of the devices' most distinguishing characteristics. Researchers from MIT and LL developed a laser radar that could generate high-resolution 3-D pictures using a small amount of light by employing a focal-plane array of 32 32 GMAPDs with independent digital time-of-flight counting circuits at each pixel. This was accomplished by using a low amount of light. Figure 2.17 displays a snippet of the output that was generated by Jigsaw. A target that was obscured by vegetation may be seen once the range of the point cloud in the laser radar's 3D view is cropped.

In 2010, an unique use of three-dimensional laser radar was shown for usage in gaming consoles. The original Kinect, which was a motion detecting device, utilized the triangulation method in order to arrive at its distance calculations. In 2012, a time-of-flight-based implementation of Kinect for Windows based on the time-of-flight technique was made available. It does this by calculating the relative phase shift between the sent signal and the received signal using a number of different sensors in order to detect whether or not the signals are locked in phase. LEDs are capable of emitting light in the near-infrared region, and this light's intensity may be modulated using a sine function or another periodic function. The sensor collects four samples at regular intervals from each pixel, with each sample being uniformly spaced apart, so that it may evaluate the phase of the scene concurrently. A technique for phase demodulation known as "four-bucket sampling" can be used to calculate the distance between the sensor and the target item. The so-called smart pixels on a CMOS chip are used as the sensor, and the distance between each pixel and the scene is measured in a manner that is independent of the others. Compared to the Swissranger SR3000 and SR4000 cameras, the PMD CamCube camera has 204 × 204 pixels, while both of those cameras have 176 x 144 pixels [66].

Research on the phenomenon of foliage peeking through has also been carried out in other places. Gronwall et al. [67] proposed a sequential technique for recognizing and identifying manmade things in environments that are dominated by natural vegetation by making use of the data collected by three-dimensional laser sensors. Armbruster150 discusses some examples from helicopter obstacle avoidance, object detection in surveillance applications, object recognition at high range, multiobject tracking, and object reidentification in range picture sequences in relation to the use of range imaging. Some of the examples come from helicopter obstacle avoidance, object detection in surveillance applications, object recognition at high range, and multiobject tracking. He claims that the automatic target recognition (ATR) capabilities of 3-D laser radars may outpace not only the skills of 2-D laser radars but even the eyesight of humans.

Another effort in the United States with the objective of "developing and demonstrating the capacity to offer precise geolocation of ground targets linked with high-resolution 3-D imagery at practical standoff ranges" was called the SPI 3-D program. In order to attain these dual capabilities, a sensor package that was already on the market was utilized. It has the potential to see through light foliage and see through the smoke caused by small weapons fire. Additionally, it may deliver "optical quality precision at radar standoff ranges."

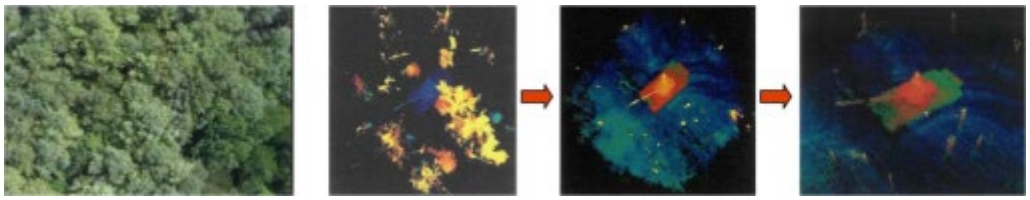

Figure 2.17: Here is an Example of Jigsaw Data Showing The Location of a Tank Target Hidden Among Trees.

2.9 THZ RECTANGULAR MICROSTRIP PATCH ANTENNA

Laser Detection and Ranging (also known as LADAR), optical free space communication, holographic displays, optical trapping, and a great deal of other applications are all possible when optical antennas are used in an optical phased array. The identification of several neurotransmitters crucial to brain activity has demonstrated that the THz technique is potentially valuable for understanding brain activities in a variety of contexts [68]. In

particular, this identification has demonstrated that the THz technique is potentially useful. One of the many tangible benefits that come from utilizing the THz range for satellite and indoor wireless communication systems is the ability to make use of transmitting and receiving antennas that are both robust and compact. This is just one of the numerous advantages that this range offers. When it comes to point-to-point communications across short distances that need a high data throughput (Gb/s to Tb/s), THz lines are probably the most secure option [69]. Optical antennas are required for a wide variety of applications, including radio astronomy [70], on-board satellite links, missile radar, inter- and intra-orbital communications, communications within a space vehicle, the Global Positioning System (GPS), satellite, and indoor wireless communications. THz systems are becoming increasingly ubiquitous in a variety of scientific domains, but their widespread application has been impeded since there is a paucity of widely available, tiny light sources. There have been a lot of attempts made to produce practical THz-frequency sources, but as of right now, there aren't any sources like that [71]. This is because there are concerns with the size, output power level, and operating temperature.

2.10 CONCLUSION

Laser radars have gone through numerous stages of development since the first attempts to use lasers for ranging. Laser designation, which is a sort of bistatic laser radar, has found considerable usage in the military for range finding and missile guidance. Research has advanced to the point that 3-D laser imaging systems are now being fielded. These systems have evolved from 2-D gated viewing systems during the course of the research that has been conducted. Imaging system innovations are currently being developed to improve weather penetration, see through vegetation and dense media, identify targets, and perform a variety of other tasks. Some of these innovations include multispectral or broad spectral emitting lasers, single-photon sensitive arrays, and improved range and cross-range resolution. Other innovations include multispectral or broad spectral emitting lasers [72].

3. METHODOLOGY

3.1 PROPOSED SOLUTION

An effective design for a THz optical antenna that might be used in screening, optically pumped terahertz lasers, video rate imaging systems, and homeland security has been presented. The substrate of the antenna in this study is made of polyimide, which has a dielectric constant of 3.5, making it possible for the antenna to function at THz frequencies. This is a novel approach to antenna design. The substance that makes up the host substrate has a low dielectric constant and a low relative permittivity. The proposed antenna has many useful applications in the real world, some of which are listed below: screening (at frequencies between 0.2 and 4 THz) [73], transistors (at frequencies between 0.48 and 0.68 THz) [74], a video rate imaging system (at frequencies between 0.6 and 0.8 THz) [75], and homeland defense (at frequencies between 0.6 and 0.8 THz) [76].

3.2 CST STUDIO SUITE

CST Studio Suite® is unparalleled in its ability to design electromagnetic (EM) components and systems as well as perform electromagnetic analysis and optimization.

CST Studio Suite gives users access to electromagnetic field solvers across a broad variety of electromagnetic (EM) applications through the use of a common interface. Engineers now have additional options available to them when it comes to the analysis of complicated systems that consist of a great number of components since the solvers may be utilized for hybrid simulations. EM simulation has the potential to be included into the design flow by making use of co-design with other SIMULIA tools. This would result in early-stage development guidance being provided.

In the discipline of electromagnetics, some of the most popular topics of research are the efficiency and performance of antennas and filters, EMC and EMI, human exposure to electromagnetic fields, electro-mechanical effects in motors and generators, and thermal effects in high-power devices.

CST Studio Suite is used by a significant number of the most famous technology and engineering companies in the world. It makes it possible to have shorter development cycles and reduced expenditures, which are both big benefits in terms of getting things to market much more quickly. The use of simulation allows for the creation of digital models that function as prototypes. There are a number of potential outcomes that might result from using such an approach, including the optimization of device performance, the early discovery and resolution of potential compliance concerns, a reduced requirement for physical prototypes, a lower probability of test failures, and fewer recalls.

3.3 DESIGN OF THE PROPOSED ANTENNA

3.3.1 Microstrip Patch Antenna

In addition to its many other advantages, the patch antenna has an emission pattern that is suited for usage in two-dimensional arrays due to its broadside orientation. The antenna has a low cost, a compact footprint, a high degree of conformability, and is straightforward to manufacture. The incorporation of microstrip or coaxial probe feeding is a simple process. Multilayer systems have a wide range of applications, some of which include CPW and strip line feeding, to name just two. Utilizing microstrip feeding allows for a straightforward realization of either linear or circular polarization excitation of the antenna [74].

The patch antenna is a typical example of a planar antenna, and it receives its power supply from a microstrip, as can be seen in Figure 3.1. The feeding of the patch antenna has an effect on the ripple, as well as the levels of cross-polarization, as well as the bandwidth. In most cases, microstrip-fed patches have bandwidths that are lower than 5%. Other feed approaches, such as proximity coupling and aperture coupling, have also been utilized to increase bandwidth, despite the fact that each of these techniques require multilayer manufacture. Pozar is the place to go if you want additional information regarding this technology (1992). On the other hand, the antenna's matched bandwidth may be enlarged by increasing the electrical thickness of the substrate, which will result in a decrease in the Q-factor of the antenna cavity. This change will have the opposite effect of expanding the antenna's bandwidth. On the other hand, if the surface wave causes radiation to be produced,

this can result in excessive levels of TM0 surface waves, which in turn can reduce the radiation's effectiveness and cause damage to the radiation pattern (which can occur at the edge of finite ground antennas). When high-frequency antennas are mounted on substrates with high permittivity, they commonly run into the problem of the substrate being electrically thick. This problem can result in substantial amounts of TM surface waves.

As illustrated in Figure 3.1, the input match may be obtained by inserting the microstrip feed into the antenna at a distance x. Choosing the correct b dimension allows one to create the resonant cavity that is formed by the conductor on the top plane of the construction. This causes radiation to be produced at the ends of the antenna, which may be observed as fringing fields. The behavior of this antenna may be simulated in a simple and straightforward manner by using the transmission line model. This model provides a decent approximation of the input impedance and an appropriate estimate of the resonant frequency when it is used close to the point where resonance occurs. Unfortunately, due to the patch antenna's restricted bandwidth, it is rarely a good choice for a first-pass design decision since it lacks sufficient reliability. However, it is important to note that the bandwidth does provide a useful reference point and information regarding the operation of the antenna.

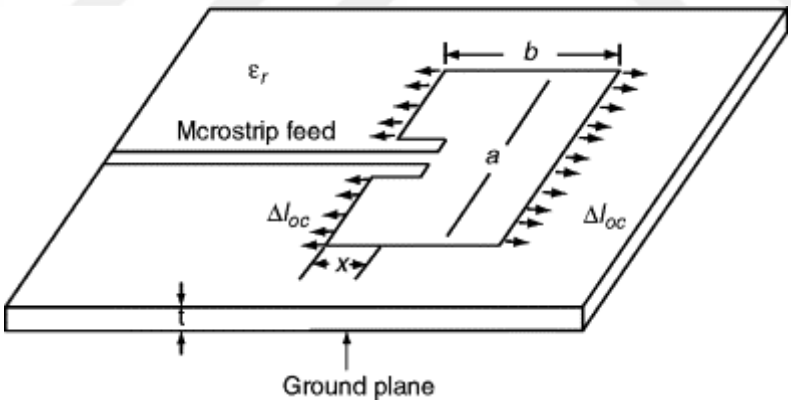

Figure 3.1: Antenna with Microstrip Feeding, Seen from Above.

The patch antenna is shown here in its cross-sectional form, which may be seen in Figure 3.2. According to this theory, standing wave type modes will arise inside the cavity of the patch antenna if the patch antenna is surrounded on all sides by walls constructed of perfect

magnetic conductor (PMC). The length of the cavity is greater than the length of the patch antenna because of the microstrip open-end phenomenon (dimension b).

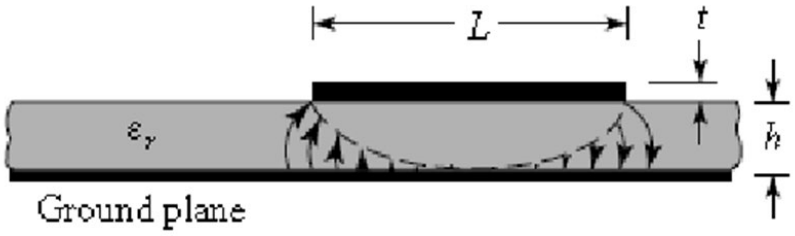

Figure 3.2: Microstrip Patch Antenna Cross Section.

The fundamental resonance of the cavity that is formed by the patch antenna will take place at a frequency at which the effective length of the patch antenna, which is equal to b plus 2loc, is equal to half of a guided wavelength in the microstrip cavity. The mathematical representation of this concept is shown below in equation 3.1.

$$f_r = \frac{c}{2\sqrt{\varepsilon_{re}}} \cdot \frac{1}{b + 2\,\Delta l_{oc}} \tag{3.1}$$

It is essential to bear in mind that the speed of light in a vacuum is c, which is equal to 3 108 meters per second, and that re is the effective permittivity of the microstrip. Equation 3.2 gives a somewhat accurate estimate of the effective permittivity by expressing it in terms of the properties shown in Figure 3.1.

$$\varepsilon_{re} = \frac{\varepsilon_r + 1}{2} + \frac{\varepsilon_r + 1}{2}\left(1 + \frac{10t}{a}\right)^{-\frac{1}{2}} \tag{3.2}$$

It is also necessary to have a rough estimation of the effective length after taking into consideration the impacts of fringing. Formulas like the one below is frequently utilized in order to determine the effective length of the fringing field (equation 3.3).

$$\frac{\Delta l_{oc}}{t} = 0.412\,\frac{(\varepsilon_{re} + 0.3)\,(^{a}/_{t} + 0.264)}{(\varepsilon_{re} - 0.258)\,(^{a}/_{t} + 0.813)} \tag{3.3}$$

Adjusting the size of the patch antenna using the aforementioned formulas allows one to get the patch antenna's desired resonance frequency. The accuracy of the model is typically

within a few percentage points at most. Because the bandwidth of a microstrip-fed patch is on the same order, this could not be accurate enough for first-pass design.

It would be nice to get an estimate of the input impedance of the antenna as well. The transmission line model of the patch antenna is the simplest and most straightforward approach to estimate this. The antenna is depicted in this image as a microstrip transmission line with the same dimensions as the patch antenna. It has two radiating slots that have the same width and length as the loc and a value, respectively. It is important to keep in mind that the feeding can be positioned anywhere along the length of the antenna when using either a coaxial probe or an inset feed.

3.3.2 Design of The Proposed Antenna

On a polyimide substrate with dimensions of 209 nm and a dielectric constant of r = 3.5, the proposed antenna was constructed. A top-down perspective of the proposed antenna arrangement may be seen in Figure 3.3. a spot of radioactive material on one. ide of substrate and ground plane on the other. ide together make up the suggested microstrip patch antenna design. The dielectric constant of the polyimide dielectric substrate is 3.5, and its relative permittivity is 3.5 as well. The design for the antenna that has been offered makes use of a copper radiating patch that has a thickness of 0.4 nanometres and measures 84 nm2 in total area. The proposed antenna receives its power through a microstrip feedline that has a width of 60 nanometres. The input impedance of the proposed antenna is 50, which is close to the impedance of the SMA connection (50), which enables the maximum amount of power to be transferred between the connector and the antenna. As can be seen in Figure 3.4, the dimensions of the ground plane of the proposed antenna are similar to those of the substrate. Figure 3.5 presents a representation of its model in three dimensions.

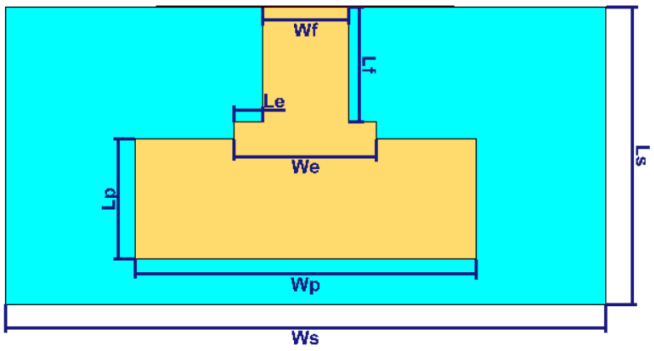

Figure 3.3: Top View.

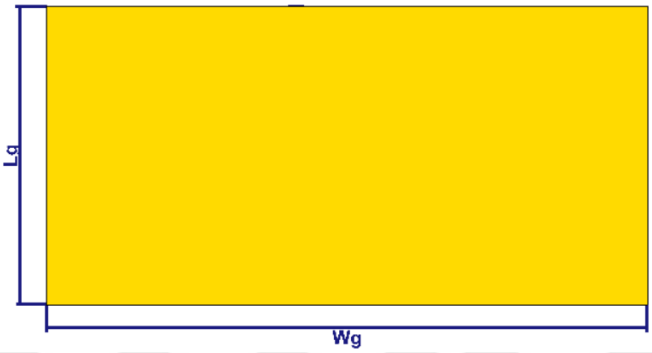

Figure 3.4: Bottom View.

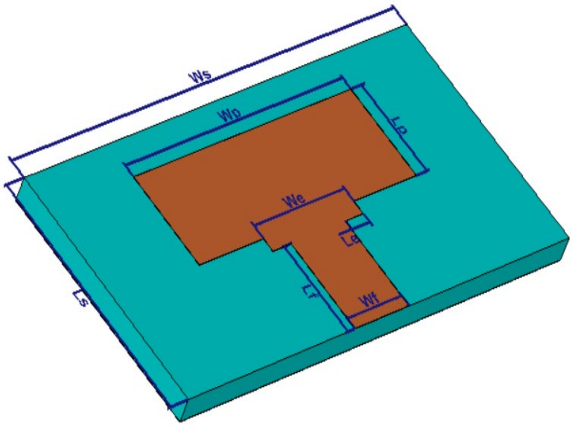

Figure 3.5: 3-D Design.

3.3.3 Antenna Dimension

In the field of wireless applications, the mentioned study [78] places a focus on the requirement for system designs that are low in cost, efficient in their use of power, and compact in size. They are in agreement that microstrip patch antennas are frequently utilised in mobile wireless communication devices due to the fact that these antennas are very inexpensive, flexible, and have a compact footprint. There are also a few drawbacks associated with using microstrip patch antennas. They are restricted in terms of bandwidth, the amount of power they can handle, gain, and directivity. Our work, which was prompted by the study that was referenced, set out to increase the functioning of microstrip patch antennas for use in ladar systems in order to overcome these limits. Our effort was motivated by the research that was cited.

In the course of our research, we fabricated a THz rectangular microstrip patch antenna by making use of a polyimide substrate that had a dielectric constant of 3.5. In the proposed design for an antenna, there was a copper radiating patch of a specified size placed in between a polyimide substrate and a ground plane of the same size. For the purposes of simulation and analysis, we relied on CST Microwave Studio 2014. This helped us confirm that our design was sound.

In conclusion, the scope of our research extends beyond the broad parameters outlined in the literature [78] and focuses on the development of improved microstrip patch antennas for ladar applications. By using a substrate made of polyimide and carefully optimising the size of the antenna, we were able to improve the impedance matching, as well as the bandwidth, gain, and directivity of the device. The practicality of employing microstrip patch antennas in ladar systems was demonstrated by our design, which was confirmed by using the modelling and analytical capabilities of CST Microwave Studio 2014.

The antenna dimensions have been tabulated in Table 3.1.

Table 3.1: Antenna Dimension.

Antenna Dimensions	**Value (µm)**
Length of the ground plane, L_g	209.00
Width of the ground plane, W_g	422.00
Thickness of ground plane	0.4
Patch length, L_p	84.00
Patch width, W_p	240.00
Thickness of the patch	0.4
Length of extended patch, L_e	12.00
Width of extended patch, W_e	100.00
Length of feedline, L_f	81.00
Substrate length, Ls	209.00
Substrate width, Ws	422.00
Thickness of substrate	20.00

4. DESIGN AND RESULTS

4.1 DESIGN IN CST

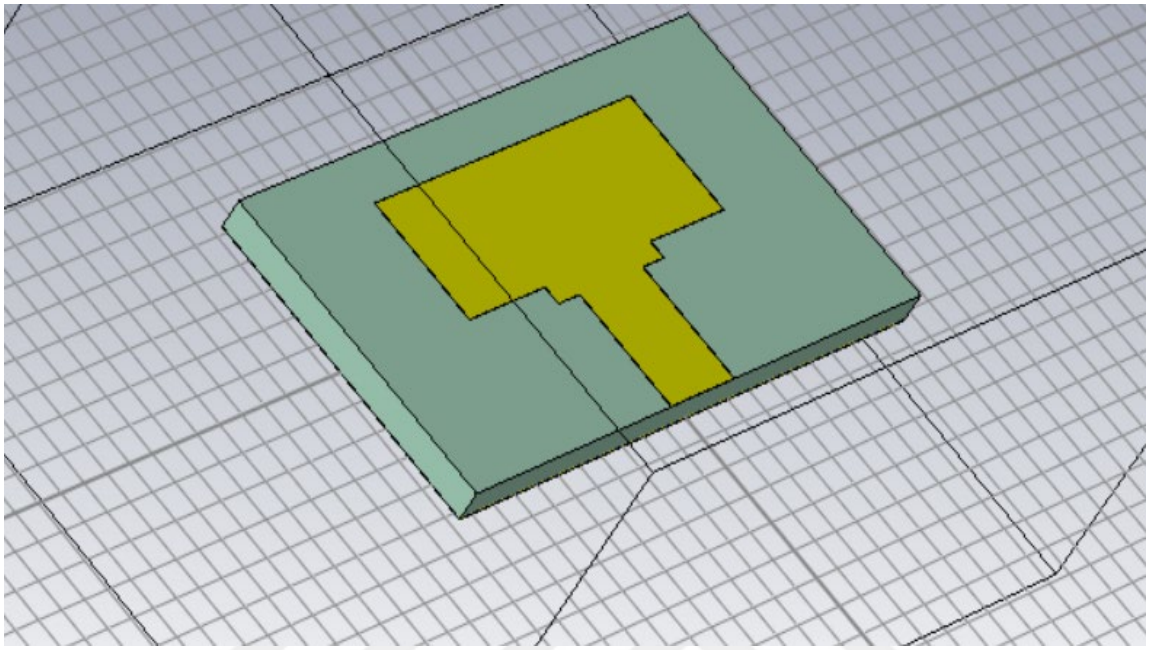

Figure 4.1: CST design View 1.

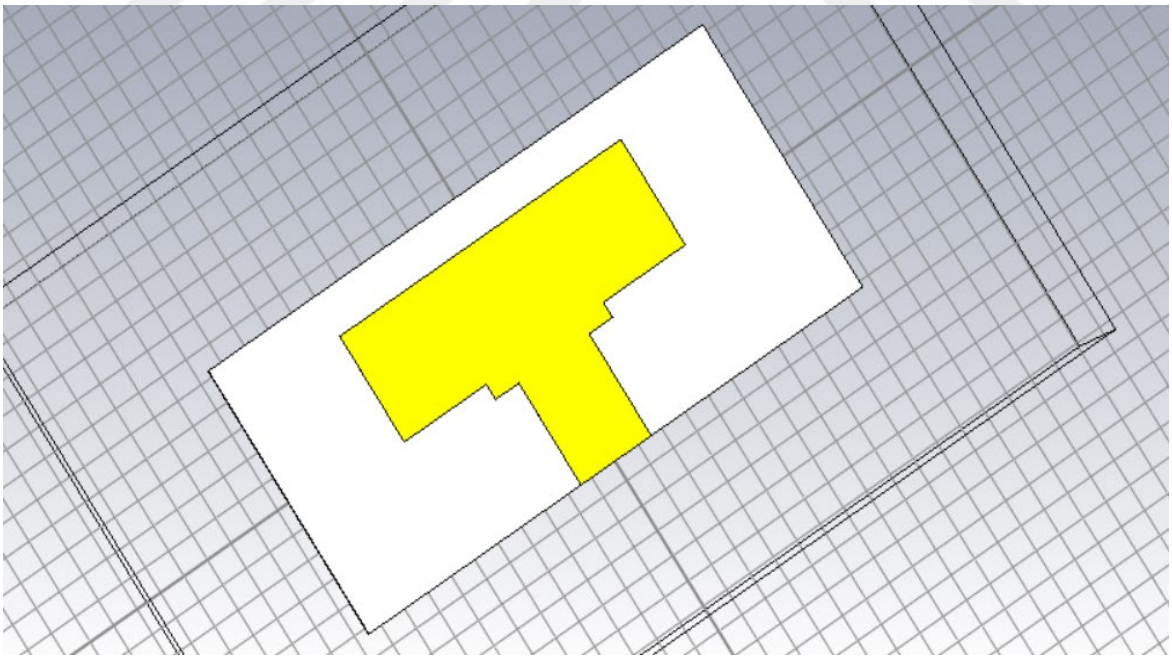

Figure 4.2: CST design View 2.

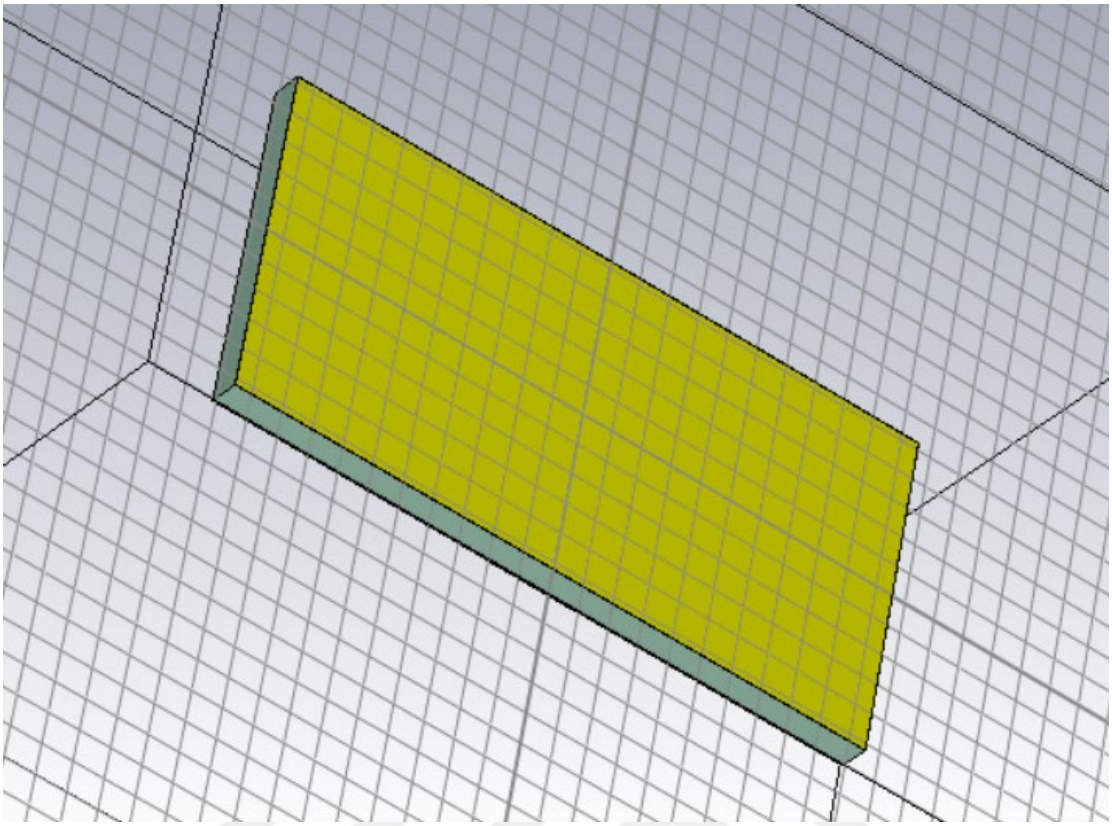

Figure 4.3: CST design View 3.

4.2 1D RESULTS

4.2.1 Port Signal

The port signal delivers the time-varying incidence (i1) and reflected (o1,1) signals on a particular port (1) to the user. In order for an antenna to exhibit strong resonance, the port signal must initially be zero and then trend toward zero both throughout and after the resonance period. Only then will the antenna be able to demonstrate robust resonance. Figure 4.4 show time-varying incidence (i1) signal and reflect good results. Same idea for time-varying reflected (o1,1) signal in Figure 4.5.

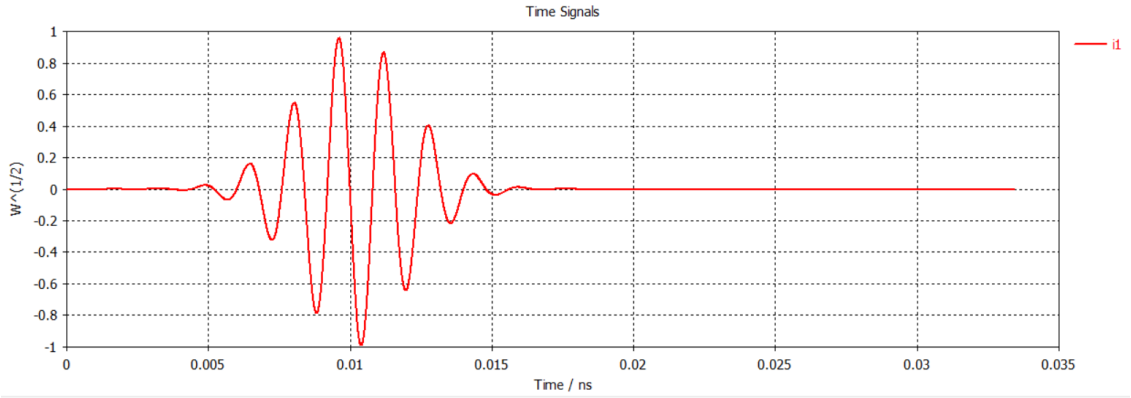

Figure 4.4: Time-Varying Incidence (i1) Signal.

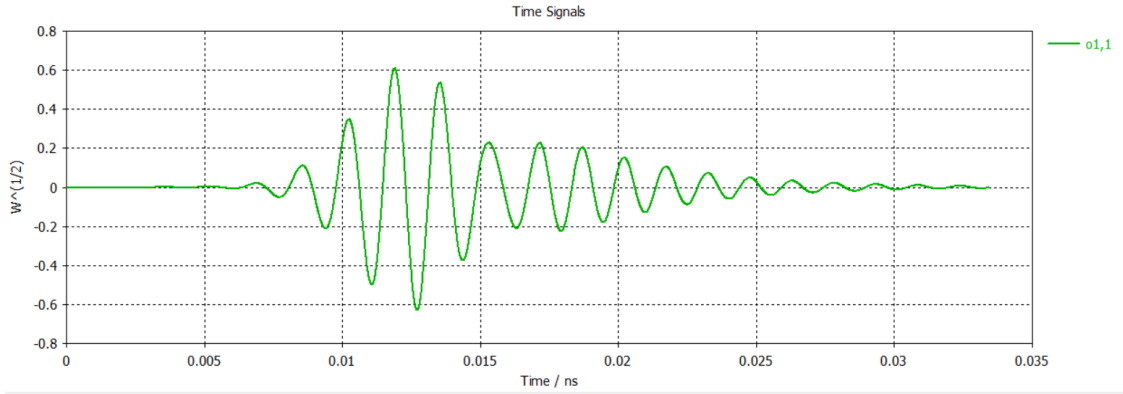

Figure 4.5: Time-Varying Reflected (o1,1) Signal.

4.2.2 S-Parameters

A group of characteristics known as S-parameters is used to characterize the connection that exists in an electrical system between the various ports (or terminals). S11 is the antenna parameter that is referenced in practice the most frequently. The sign S11 is used to indicate either the reflection coefficient of the antenna, which may alternatively be represented as gamma, or the return loss. At the point where S11 equals 0 dB, the antenna is completely reflecting all of the input energy and not producing any output. When the power going in is 3 dB, the reflected power will be -7 dB if S11 is -10 dB. The antenna either "received" the leftover energy or sent it to itself. This nominal input power is either lost as radiation or absorbed by the losses associated with the antenna. Antennas, as a general rule, are constructed such that they can radiate a maximum amount of the power that is sent into them.

As shown in Figure 4.6, at 665 GHZ, the antenna achieves a return loss of less than -16 dB with a very clean curve.

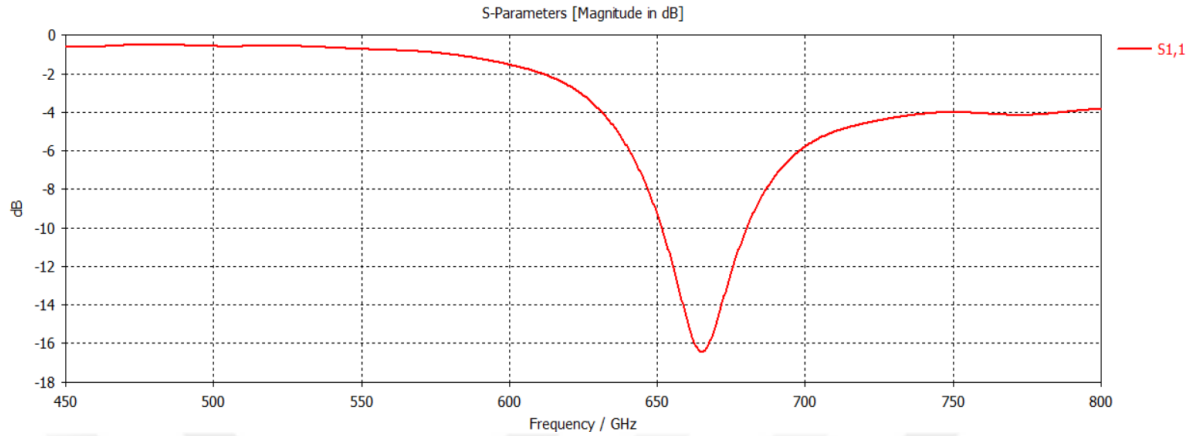

Figure 4.6: S- Parameter.

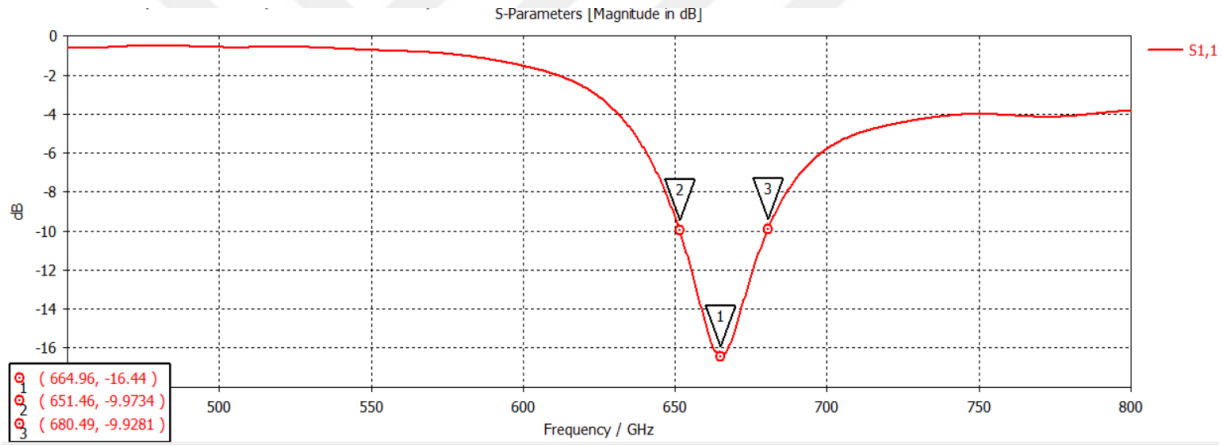

Figure 4.7: Markers.

4.2.3 Balance

It is possible to calculate the equilibrium of the S-parameter by taking the square root of the total power that is lost via the structure's outputs. The resultant balance should be 1 in all closed, loss-free (meaning there is no lumped element R) structures. (no open or lossy border condition). The power balance reveals the frequencies at which power is absorbed by the building itself or released through open borders.

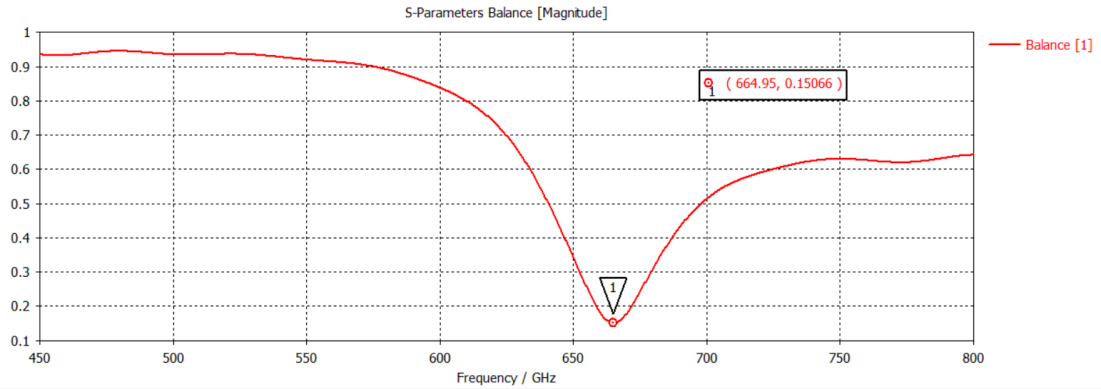

Figure 4.8: Balance Results.

4.2.4 Power

Within CST Microwave Studio's Power folder is an averaged power spectrum curve that spans all frequencies and all time periods. This curve is present throughout all time periods. This folder is located directly below the 1D Result folder and contains subfolders for every simulation that was run with a specific excitation. The names of the excitations are given by the text that is included between the square brackets. This might be a port number, the label for a simultaneous excitation, or the letters "pw" in the event that the excitation is for a plane wave.

The power that is stimulated at one or more ports is shared between the structure, which absorbs some of it, and the ports themselves, which let some of it back out (outgoing power).

In addition, a portion of the power that is absorbed is either radiated or lost (as a result of dielectrics, metals, or lumped components) (in the case of antenna applications, for instance).

Figure 4.9 show low loss and high accepted power which demonstrate the performance of the antenna.

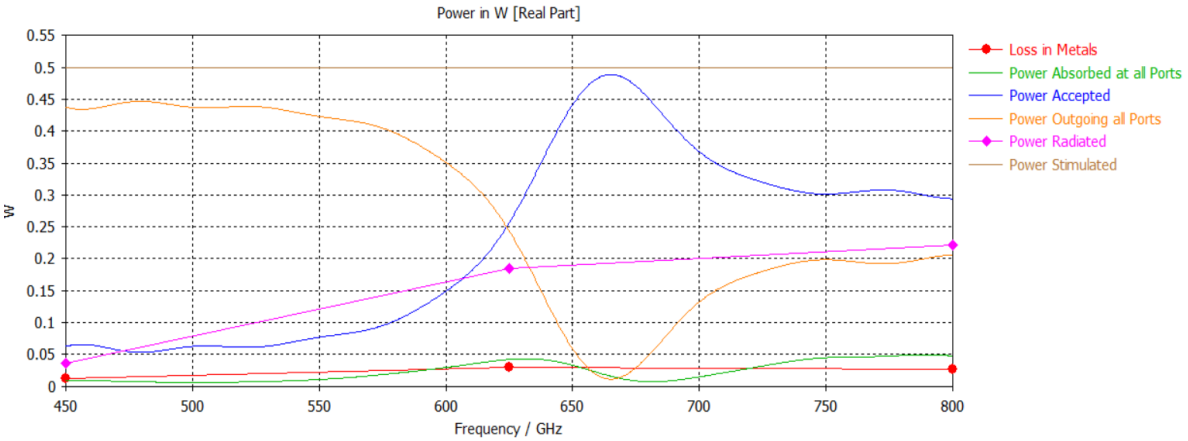

Figure 4.9: Power Results.

4.2.5 Efficiency

The Radiation efficiency at the desired frequency 72% as shown in figure 4.10, which is fairly enough.

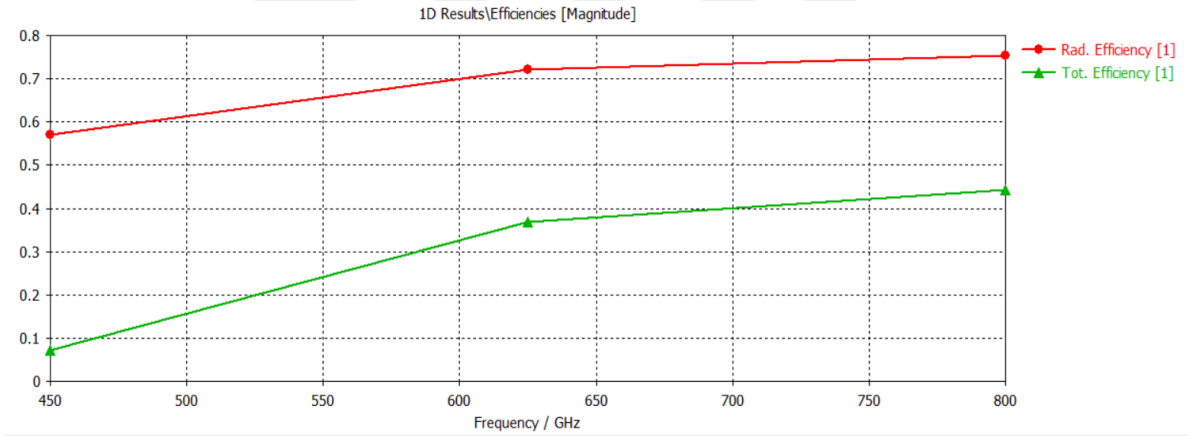

Figure 4.10: Efficiencies.

4.2.6 VSWR

It is necessary for the impedance of the radio and the transmission line to be matched to that of the antenna in order for there to be an efficient flow of energy from the radio (either the transmitter or the receiver) to the antenna. The value of the VSWR parameter can be used as a numerical indicator of how efficiently an antenna is impedance matched to the radio or

transmission line to which it is linked. This can be done by comparing the value of the VSWR parameter to a known value.

The term "Standing Wave Ratio" can also refer to "Voltage Standing Wave Ratio," which is abbreviated to "VSWR" (SWR). The magnitude of the voltage standing wave ratio has a one-to-one correspondence with the reflection coefficient, which is a measure of the power that is reflected from the antenna (VSWR).

As shown in figure 4.11, VSWR value at 665 GHz is equal to 1.3564 which is not only less than 2 the max acceptable value, it is less than 1.5 which make the antenna works well.

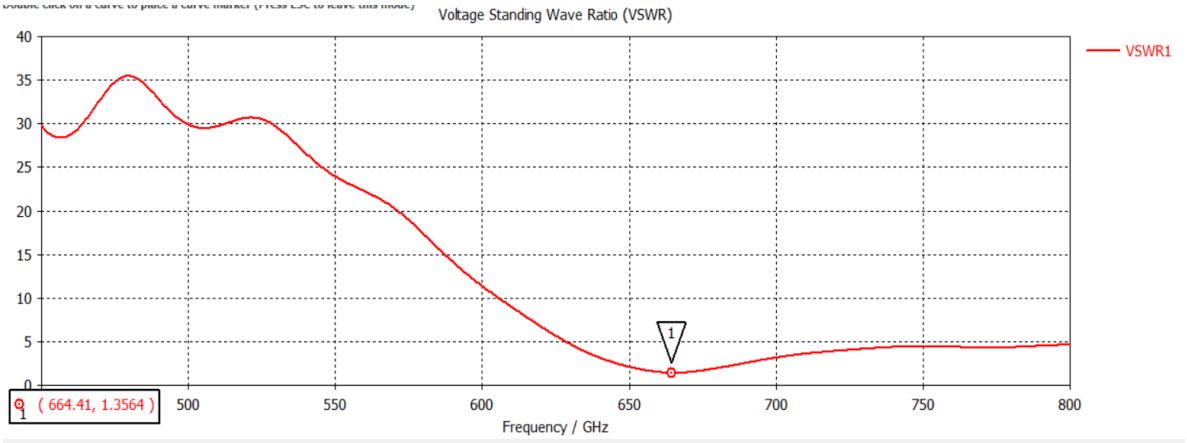

Figure 4.11: VSWR Results.

4.3 2D/3D RESULTS

4.3.1 E-Fields

An electric field is a physical field that surrounds charged particles and exerts a force on all other charged particles in the field, either attracting or repelling them depending on the direction of the force. An electric field is frequently written as E-field. A system of charged particles may also be described using this word to talk about the underlying physical field of the system. Electric fields are generated through the interaction of electric charges and alternating currents. Both electric and magnetic fields are manifestations of the electromagnetic field, which is one of the four fundamental interactions (also referred to as forces) that may be found in nature.

Electric fields are important to the study of a wide variety of physics subfields, in addition to their application in the field of electrical technology. When studying atomic physics and chemistry, for example, it is essential to have an understanding that the electric field acts as the attractive force that keeps the nucleus and electrons of an atom bound to one another. This is because the electric field keeps the nucleus and electrons of an atom in close proximity to one another. The presence of this force enables the formation of chemical bonds between atoms, which in turn permits the atoms to assemble into molecules.

The electric field is a vector field, and by definition, it assigns to each position in the universe the electrostatic or Coulomb force per unit of charge that would be exerted on an infinitesimally small positive test charge if it were to be resting at that location. Volts per meters (V/m), which in the SI system is equivalent to newtons per coulombs (N/C), are the units used to quantify the strength of the electric field.

As shown in figure 4.12, electric field does not exceed 106 dB (V/m) which make the antenna safe to use.

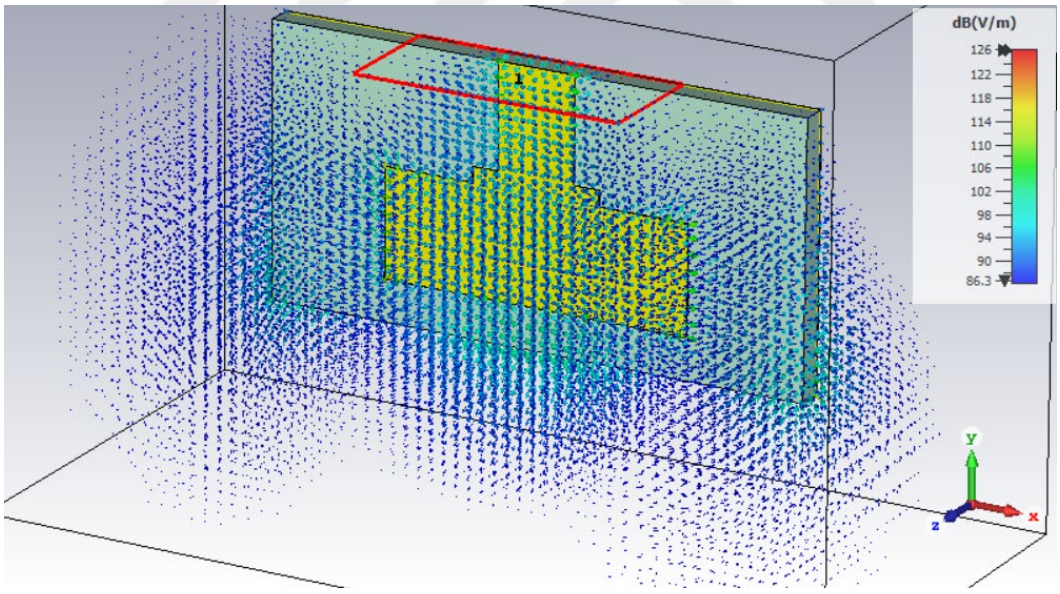

Figure 4.12: E-fields at 625 GHz.

4.3.2 H-Fields

A magnetic field is a term that refers to the vector field that is used to describe the magnetic force that is exerted on moving electric charges, electric currents, and magnetic materials. When a charge moves through a magnetic field, it is subject to a force that acts in a direction that is perpendicular to both the direction in which the charge is moving and the magnetic field. Permanent magnets produce a magnetic field that may either attract or repulsion other magnets and exert a pulling force on ferromagnetic materials like iron. Other magnets can be attracted or repelled by this field. In addition, the force of a magnetic field may be felt by a range of non-magnetic materials because of the magnetic field's impact on the velocity of the electrons in the outer shells of the atoms in such materials. This is true despite the fact that the materials lack magnetic characteristics. Magnetic fields are produced by electric currents, such as those used in electromagnets, as well as time-varying electric fields. These magnetic fields surround items that may be magnetized. A magnetic field may be described mathematically as a vector field, in which both the strength and the direction of the field are treated as independent variables.

In today's engineering and science, magnetic fields are useful in a wide variety of applications, particularly in the domains of electrical engineering and mechanical engineering. Both electric motors and generators depend on the rotation of magnetic fields in order to function. When investigating the interaction of magnetic fields in electrical equipment such as transformers, magnetic circuits offer a helpful conception and analytical tool for analysing this dynamic. The reaction of a material's charge carriers to the application of magnetic fields is what the Hall effect uses to determine. Compass navigation is impossible without the inherent magnetic field of the Earth, which also shields the ozone layer from the effects of the solar wind.

As shown in figure 4.13, magnetic field does not exceed 3000 (A/m) which make the antenna safe to use.

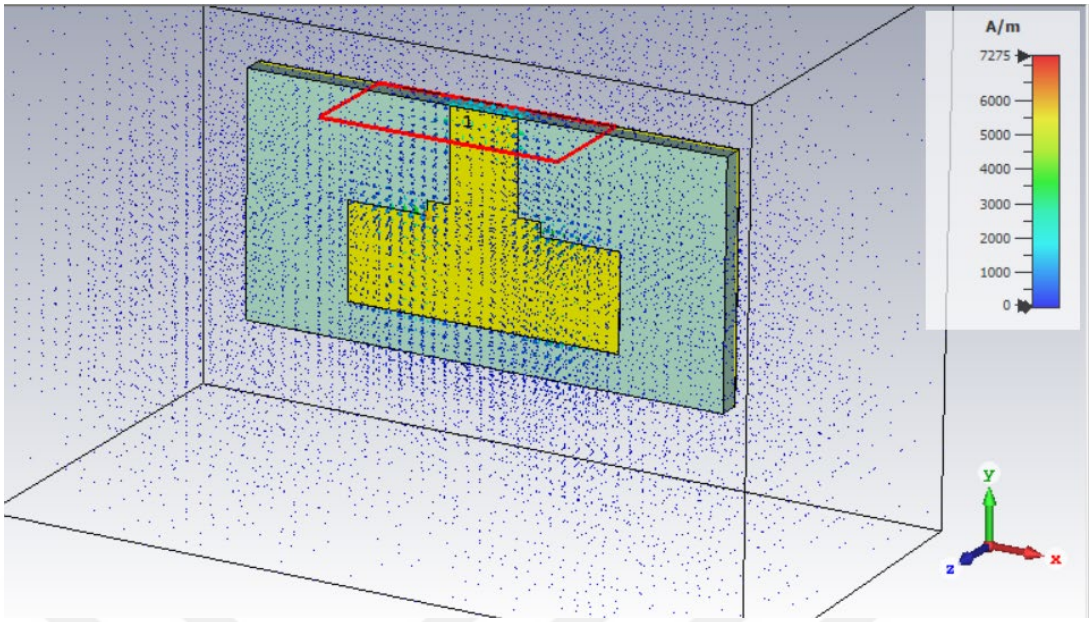

Figure 4.13: E-Fields at 625 GHz.

4.3.3 Surface Current

The idea that there is a current just below the water's surface is purely speculative at this point. In actuality, the only currents that can be identified are volume currents. The surface current of a metallic antenna is a true electric current that is created by the electromagnetic field that is external to the antenna. The electric field has the ability to move charges around in a system. Nearly any piece of simulation software that is able to represent metals will also have the ability to visualize surface currents. For instance, the concept of moments is used to compute the surface current that is flowing through conductors.

You said previously that you are interested in gaining further knowledge about dielectric antennas. Even if dielectric currents are still around, I don't think there's any use in continuing to research them. Charges can only receive the displacement current because of the limits placed on them. alterations in the manner in which charges are dispersed about their atoms. When the charges are moved in such a way, the state of the material is referred to as being polarized. It is rare for a modelling tool to display the displacement current because the permittivity of the material already takes into consideration all of these aspects.

As seen in the figure 4.14, the current is distributed smoothly on the surface.

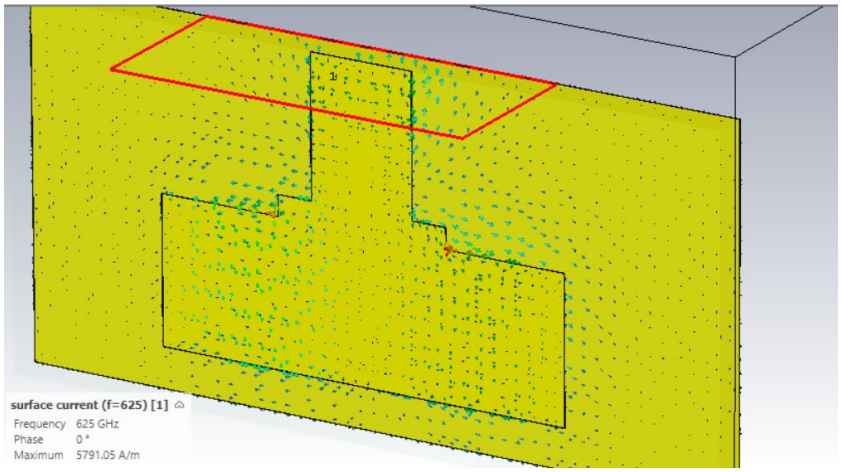

Figure 4.14: Current Surface.

4.3.4 Far-Field

2D far-field directivity is shown in figure 4.15. 3D far-field directivity at 450 GHz and 625 GHz in Figure 4.16 and 4.17 respectively.

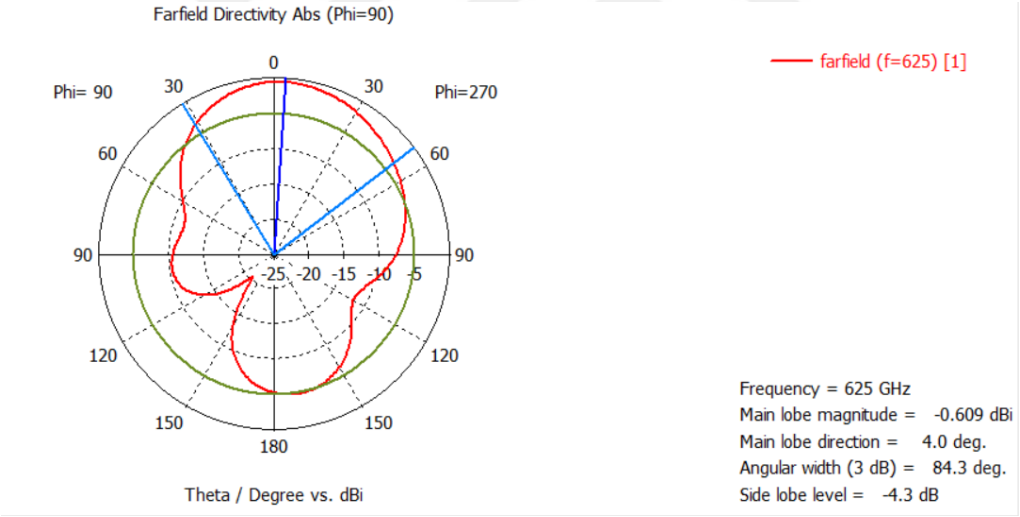

Figure 4.15: 2D Far-Field Directivity.

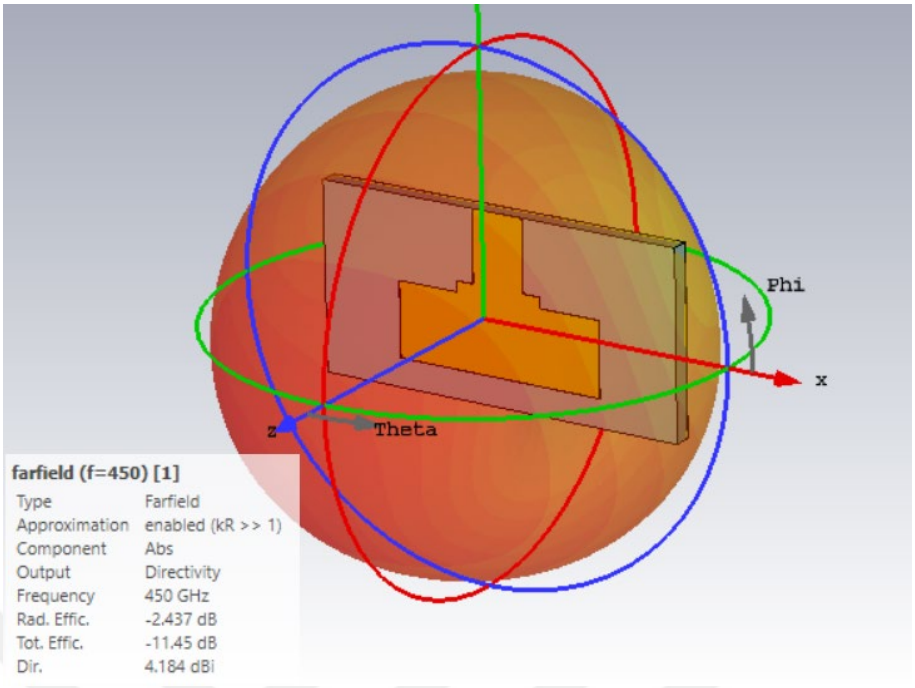

Figure 4.16: 3D Far-Field Directivity at 450 GHz.

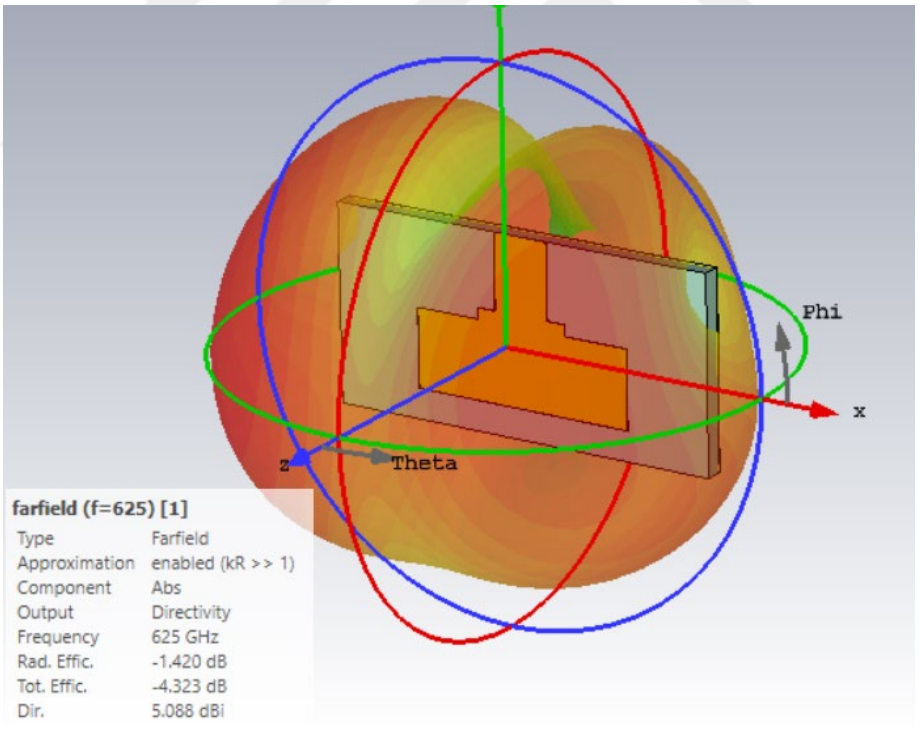

Figure 4.17: 3D Far-Field directivity at 625 GHz.

4.4 SUBSTRATE MATERIALS

Changing the substrate material allows to get different values for the dielectric constant (r). The creation of microstrip antennas has resulted in the identification of a diverse collection of substrate materials.

In this study, the performance of the same antenna is compared on substrates made from FR4, Rogers RO3003, Rogers RO4725JXR, Taconic CER-10, and Polyimide, with dielectric constants of 4.0, 3.6, 10.0, and 3.5, respectively. These materials were chosen because of their high frequency response and low loss. The return loss parameter is utilized in the process of evaluating the performance of the antenna with respect to a wide variety of substrate materials. At CST studio, similar antennas are fabricated and put through their paces of testing. In Table 4.1, an overview of how the parameters of the antenna are affected by the various substrate materials is provided. According to Table 4.1, the reflection offered by polyimide is of the best possible quality. Figure 4.18 illustrate all results.

Table 4.1: Substrate Material Variation.

Material	ε_r	**Frequency peak (GHz)**	**S11 (dB)**
FR4	≈ 4.0	622.92	-14.08
Rogers RO3003	3	718.25	-13.48
Rogers RO4725JXR	2.64	764.98	-12.38
Taconic CER-10	10.0	765.35	-8.31
Polyimide	3.5	664.14	-16.47

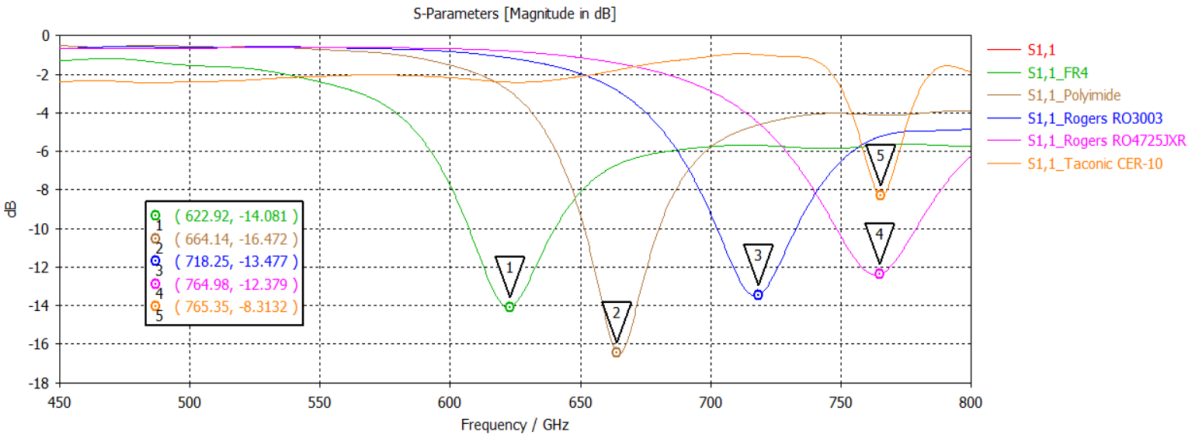

Figure 4.18: Substrate Material Variation.

4.5 PATCH WIDTH VARIATION

In this section, a study about the effect of the patch width is provided. Table 4.2 shows the 241 mm works the best for this design (See Figure 4.19).

Table 4.2: Variation in Patch Width.

Width	**Size (mm)**	**Frequency peak (GHz)**	**S11 (dB)**
W	240	664	-16.45
W1	238	670.09	-14.77
W2	242	661.82	-17.33
W3	241	660.75	-18.47

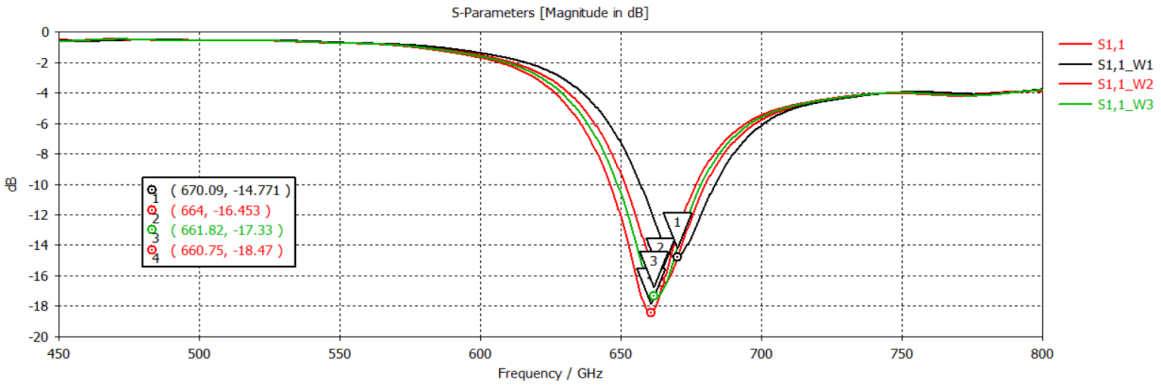

Figure 4.19: Width of Patch Effect.

4.6 FEEDLINE WIDTH VARIATION

The feedline width affects the return loss and results of the antenna as shown in table 4.3 and Figure 4.20. 56 mm was the best width.

Table 4.3: Feedline Width Variation.

Width of feedline	**Size (mm)**	**Frequency peak (GHz)**	**S11 (dB)**
F	60	664	-16.45
F1	58	665.33	-16.735
F2	62	664.91	-16.188
F3	56	665.45	-17.159

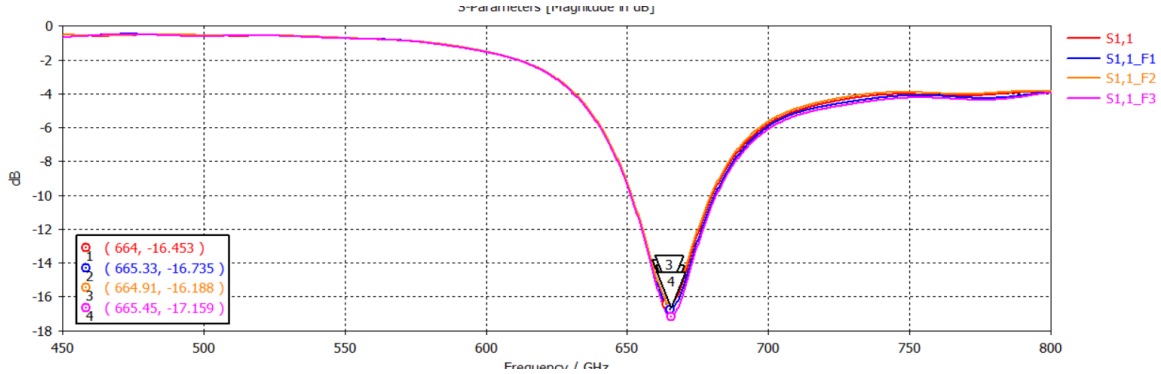

Figure 4.20: Feedline Width Effect on Return Loss.

4.7 FEEDLINE NOTCH WIDTH VARIATION

In this design, a small notch was designed to be 100 mm. Some variation on its width affects positively the return loss. Table 4.4 shows that 96 mm notch width works the best (Figure 4.21).

Table 4.4: Feedline Width Effect.

Width of feedline notch	Size (mm)	Frequency peak (GHz)	S11 (dB)
N	100	664	-16.45
N1	98	664.72	-16.72
N2	102	665.23	-16.28
N3	96	664.59	-16.841

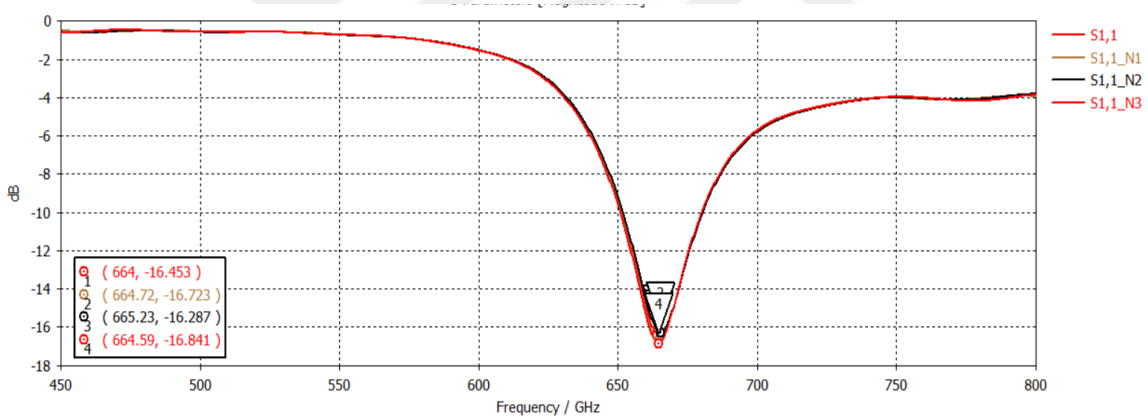

Figure 4.21: Feedline Width Effect.

4.8 MODIFIED VERSION

Collecting all data, a modified version of the antenna is tested, where polyimide substrate is used with a 241 mm patch width, 56 mm feedline width and 96 mm notch width. It gives at 663.46 GHz a -18.545 dB return loss (Figure 4.22).

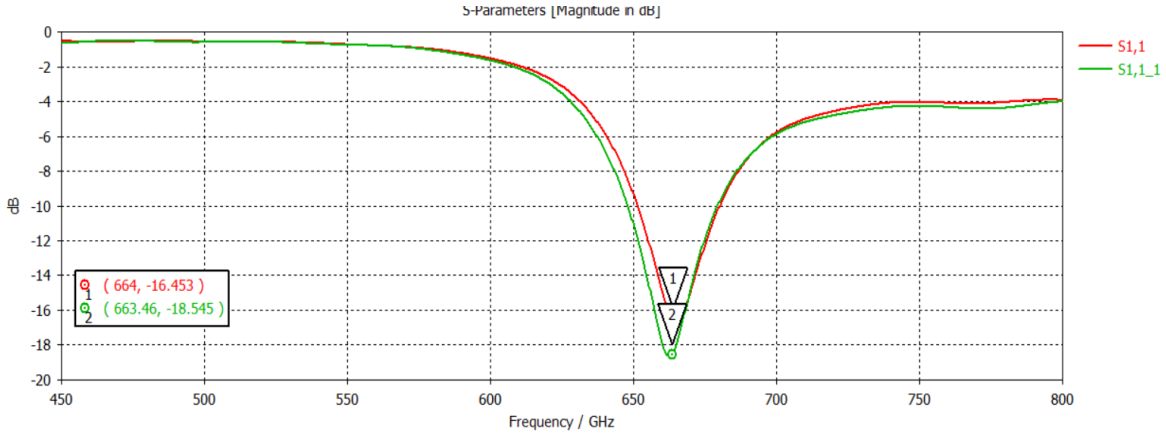

Figure 4.22: Final Return Loss Results.

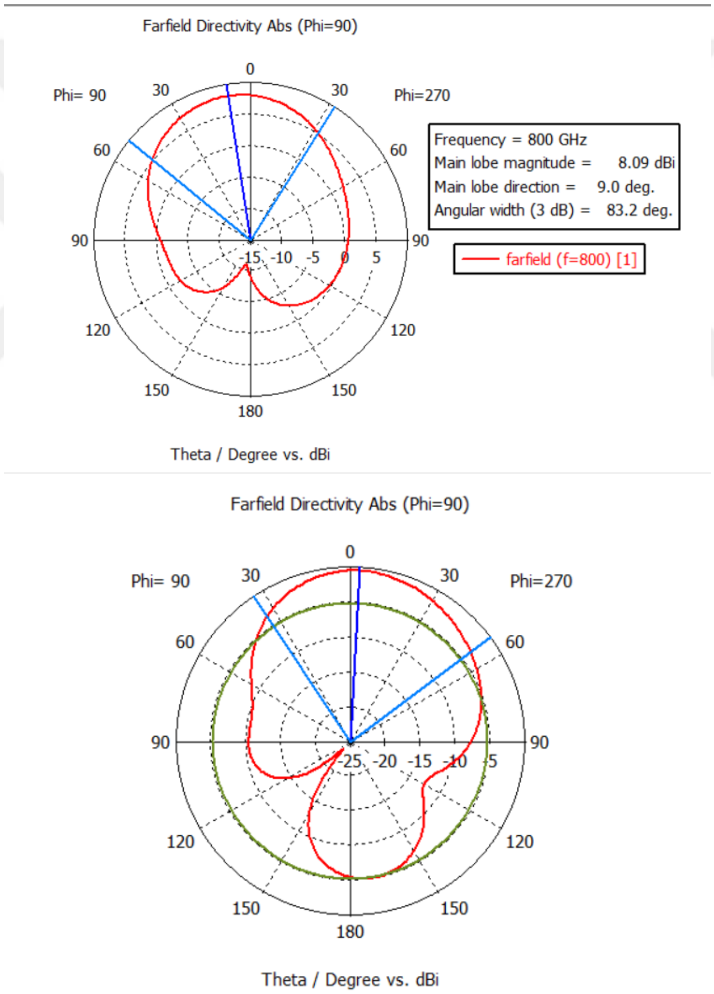

Figure 4.23: Fairfield.

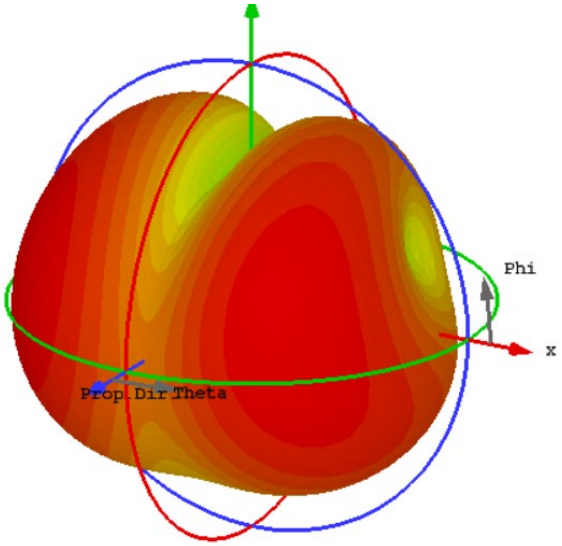

Figure 4.24: Gain 3D.

4.9 COMPARISON

In the study that was referenced [78], an optical rectangular patch antenna operating at THz frequencies and constructed out of polyimide was demonstrated. Their design, which utilizes a polyimide substrate with a dielectric constant of 3.5, demonstrates antenna characteristics such as impedance bandwidth, directivity, gain, return loss, and VSWR. These characteristics are all illustrated by the antenna itself. The conductivity and resistance of the various components of the antenna's feedline, radiating patch, and ground are all distinct from one another. The feedline is comprised of copper (Cu). It has a gain of 5.22 decibels and a directivity of 5.08 decibels when it is operating at its resonance frequency of 0.67 THz. The impedance bandwidth is 40.16 GHz, and it spans the frequency range of 0.65 THz to 0.69 THz.

Our work, on the other hand, provides an original design for a square antenna that may be used for wireless communications in the frequency range of 2.33 to 12.4 GHz. These antennas have the potential to be beneficial for wideband license-free communications (UWB). We make use of microstrip patch antennas developed particularly for ladar, as opposed to the conventional antennas that were utilized in the work that was referenced. When designing a THz rectangular microstrip patch antenna, we recommend using the use

of a polyimide substrate that has a dielectric constant of 3.5. Our antenna has the capability of picking up signals with a frequency range of 0.648 THz to 0.68 THz, making it applicable to a broad variety of different areas. A resonant frequency of 0.8 THz and a directional gain of 8.09 dBi are some of the factors that contribute to the improved performance.

Furthermore, the impedance bandwidth of our design is 30 GHz, which enables us to cover a greater variety of frequency ranges than the study that was mentioned. When the matching circuit is improved, our antenna demonstrates substantially superior impedance matching with a return loss of just -18.632 dB at the resonance frequency of 0.625 THz. This indicates that the matching is quite good.

Our research and the research that was quoted both point to the possibility of application in video rate imaging systems (at 0.6 THz) and in homeland security (at 0.6 THz to 0.8 THz). The performance of our design, on the other hand, is superior to that of its competitors in important areas such as the operating frequency range, gain, and impedance matching. As a result of these enhancements, our proposed design for a square antenna is now a more viable alternative to the polyimide-based optical rectangle patch antenna that was utilized in the referenced paper for the purpose of improving the performance of wireless communication within the specified frequency range. Studies [79-81] have presented fare results, however, the frequencies are not suitable for this study application.

For more comparison, table 4.5 shows some similar work. It is clear that for such application the proposed design plays the best solution.

Table 4.5: Comparison.

	Peak Frequency (THz)	**Range**	**S11**
Dual Band THz Antenna Using T Structures and Effect of Substrate Volume on Antenna Parameters [75]	0.63	0.60-0.65	-17
Liquid Crystalline Polymer Substrate-Based THz Microstrip Antenna Arrays [76]	0.835	0.82-0.84	-30
a Broadband U-Shaped Microstrip Patch Antenna on Silicon-Based Technology for 6G Terahertz (THz) [77]	0.3	0.279-0.305	-14.9
THz 2-D Frequency Scanning Planar Integrated Array Antenna with Improved Efficiency [78]	0.33	0.325–0.4	-35
Design of MEMS on-chip helical antenna for THz application [79]	3.3	2.8-4.4THz	-30
A 0.55 THz On-Chip Substrate Integrated Waveguide Antenna [80]	0.55	0.54 - 0.56	-35
Our proposed design	0.663	0.648-0.679	-18.632

4.10 CONCLUSION

There is a proposition for a THz rectangular microstrip patch antenna. The substrate material would be polyimide, and it would have a dielectric constant of 3.5. This would enable the antenna to function in the frequency range of 0.648 THz to 0.68 THz. When utilizing the antenna that was proposed, resonance happens at a frequency of 663 gigahertz. The proposed antenna has a directional gain of 8.09 dBi, and its resonance frequency is calculated to be 0.8 THz. The impedance bandwidth of the antenna is 30 gigahertz. At the matching resonance frequency of 0.625 THz, the modelled antenna was tested to have the lowest return loss possible, which was -18.632 dB.

5. CONCLUSION

5.1 CONCLUSION

Although patch antennas are commonly employed in some situations, they possess certain inherent limitations such as a relatively low gain factor and a restricted bandwidth. The widespread acceptability of [something] has experienced a drop as a result of these limitations. The key objectives of developing these antennas have been to boost broadband capabilities and improve signal strength. This correspondence presents an examination of a novel square patch antenna, which exhibits promising capabilities for significantly augmenting wireless communication within the frequency range of 2.33 to 12.4 GHz. The augmentation of available spectrum, particularly within the ultra-wideband (UWB) realm, aligns with the objective of facilitating unlicensed communications with broad frequency ranges. The formal recognition of the ultra-wideband (UWB) spectrum by the United States Federal Communications Commission (FCC) occurred in 2002. This spectrum encompasses a frequency range of 3.1 GHz to 10.6 GHz. Moreover, the microstrip patch antenna has gained significant popularity for applications involving high frequencies.

This dissertation aims to establish a comprehensive framework for antenna design utilising microstrip patch technology, with a specific emphasis on its applications in laser radar (ladar). The thesis is composed of five distinct components. The initial chapter provides a comprehensive overview of the research's contextual background, challenges encountered, and anticipated contributions, so outlining the essence of the study. The subsequent phase involves conducting a comprehensive literature review that situates the study within the broader framework of prior investigations pertaining to laser radar systems, while also evaluating the extent to which they align with the research goals.

Chapter 3 provides a comprehensive analysis of potential applications for the developed model, while the subsequent chapter delves into the methodology employed in its creation. The findings of the research are reported and analysed in the fourth chapter. The data acquired is presented and analysed in this section.The use of polyimide as the substrate material, together with a dielectric constant of 3.5, is proposed in the thesis. Additionally,

the thesis recommends the implementation of a rectangular microstrip patch antenna designed to operate within the terahertz (THz) frequency range. The resonance frequency of the antenna is measured to be 674 GHz, while its operational frequency range spans from 0.648 to 0.68 terahertz. The directional gain of the antenna is measured to be 8.09 decibels relative to an isotropic radiator (dBi), indicating its ability to focus and amplify electromagnetic signals in a specific direction. Additionally, the antenna exhibits resonance at a frequency of 0.8 terahertz (THz), indicating its optimal performance at this particular frequency. The impedance bandwidth of the system encompasses a frequency range of 30 GHz. The simulated antenna has a notable return loss of -18.632 dB at the resonance frequency of 0.625 THz, suggesting a high level of efficiency in the matching circuit.

The suggested antenna design has the potential to be utilised in several applications, including but not limited to lidar, imaging systems operating at a video rate of 0.6 THz, and homeland security applications within the frequency range of 0.6-0.8 THz. The antenna was developed and modelled with the state-of-the-art software, CST Microwave Studio.

5.2 FUTURE WORK

The minimal return loss and impedance bandwidth of the antenna are both projected to reduce drastically as the substrate's width expands. Our future study may focus on how altering the substrate's width impacts the antenna's percentage bandwidth and how it affects the return loss of the antenna.

REFERENCES

[1] P. Mamidipudi and D. Killinger, "Optimal detector selection for a 1.5 micron KTP OPO atmospheric lidar", Proc. SPIE 3703, pp. 327-335, 1999.

[2] T. Kobayashi, Y. Enomoto, D. Hua, C. Galvez and T. Taira, "A compact eyesafe lidar based on optical parametric oscillators for remote aerosol sensing" in Advances in Atmospheric Remote Sensing with, Berlin:Springer Verlag, pp. 11-14, 1996.

[3] William Cottingame, Project CLEAR manuscript in press, [online] Available: bill@cottingame.com.

[4] L. Williams, Wei Gong, D. A. Temple, A. H. Omar and J. Mangana, "An aerosol lidar model program used for the Center for Lidar and Atmospheric Sciences Students lidar system," IEEE International Geoscience and Remote Sensing Symposium, 2002, pp. 2291-2295 vol.4, doi: 10.1109/IGARSS.2002.1026522.

[5] O. Steinvall, "3-D imaging laser radars: modelling and experimental results," Conference Digest. 2000 Conference on Lasers and Electro-Optics Europe (Cat. No.00TH8505), 2000, pp. 1 pp.-, doi: 10.1109/CLEOE.2000.909693.

[6] S Der, B Redman and R. Chellappa, "Simulation of error in optical radar range measurements [J]", Applied optics, vol. 36, no. 27, pp. 6869, 1997.

[7] Ove Steinvall, "Range accuracy and resolution for laser radars [J]", Proceedings of SPIE - The International Society for Optical Engineering, vol. 5988, pp. 73-88, 2005.

[8] D.L. Donoho, "Compressive sensing", IEEE Transactions on Information Theory, vol. 52, pp. 1289-1306, 2006.

[9] E J. Dandes, "Near-optimal signal recovery from random projections[J]", Universal encoding strategies IEEE Transactions on Information Theory, pp. 52, 2006.

[10] E J Candes, J Romberg and T. Tao, "Robust uncertainty principles: exact signal reconstruction from highly incomplete frequency information[J]", IEEE Transactions on Information Theory, vol. 52, no. 2, pp. 489-509, 2006.

[11] G A Howland, P B Dixon and J C. Howell, "Photon-counting compressive sensing laser radar for 3D imaging[J]", Applied Optics, vol. 50, no. 31, pp. 5917-20, 2011.

[12] M J Sun, M P Edgar, G M Gibson et al., "Single-pixel three-dimensional imaging with time-based depth resolution[J]", Nature Communications, vol. 7, pp. 12010, 2016.

[13] G. W. Kamerman, “3D imaging laser radar,” 27 http://www.spie.org/conferences-and-exhibitions/defense--commercial-sensing/defense--security.

[14] V. V. Molebny, Optical Radar Systems: Basics of Functional Layouts (in Russian), 183 Mashinostroenie, Moscow (1981).

[15] M. S. Malashin, R. P. Kaminskiy and Y. B. Borisov, Basics of Laser Radar System Design (in Russian), 208 Vysshaya Shkola, Moscow (1983).

[16] I. N. Matveev et al., Laser Radar Technology (in Russian), 272 Mashinostroenie, Moscow (1984).

[17] P. F. McManamon, Field Guide for Lidar, 168 SPIE Press, Bellingham, Washington (2015).

[18] P. F. McManamon, Laser Radar. Progress and Opportunities in Active Electro-Optical Sensing, The National Academies Press, Washington, DC (2014).

[19] V. V. Molebny, Optical Radar, (in Russian), 183 Kiev University Press, Kiev (1981).

[20] R. R. Reibel et al., “Ultrabroadband optical chirp linearization for precision length metrology applications,” Opt. Lett., 34 3692 –3694 (2009). http://dx.doi.org/10.1364/OL.34.003692 AASTCFOPLEDP 0094-57650146-9592.

[21] J. M. Vaughan et al., “Coherent laser radar in Europe,” Proc. IEEE, 84 (2), 205 –226 (1996). http://dx.doi.org/10.1109/5.482229 IEEPAD 0018-9219.

[22] P. McManamon, G. Kamerman and M. Huffaker, “A history of laser radar in the United States,” Proc. SPIE, 7684 76840T (2010). http://dx.doi.org/10.1117/12.862562 PSISDG 0277-786X.

[23] V. Molebny, P. Zarubin and G. Kamerman, “The dawn of optical radar: a story from another side of the globe,” Proc. SPIE, 7684 76840B (2010). http://dx.doi.org/10.1117/12.850086 PSISDG 0277-786X

[24] V Molebny, G. Kamerman and O. Steinvall, “Laser radar: from early history to new trends,” Proc. SPIE, 7835 783502 (2010). http://dx.doi.org/10.1117/12.867906 PSISDG 0277-786X.

[25] T. Kobayashi, “Overview of laser remote sensing technology for industrial applications,” Industrial Applications of Laser Remote Sensing, 3 –15 Bentham Science Publication, Sharjah, United Arab Emirates (2011).

[26] H. Hu and J. Qiu, “An overview of lidar study in China,” Rev. Laser Eng., 3 (2), 85 – 88 (1995). REKEDA 0387-0200

[27] A. A. Lebedev, “Optics herald,” Rozhdestvensky Opt. Soc. Bull., 145 11 –15 (2014).

[28] P. A. Forrester and K. F. Hulme, “Laser range finders,” Opt. Quantum Electron., 13 259 –293 (1981). http://dx.doi.org/10.1007/BF00619793 OQELDI 0306-8919

[29] V. P. Ponomarenko and A. M. Filachev, Infrared Techniques and Electro-Optics in Russia: A History 1946–2006, SPIE, Bellingham (2007).

[30] “Weapons and technologies in Russia. XXI century,” Electro-Optical Systems and Laser Technologies, 11 720 Oruzhie i Tekhnologii, Moscow (2005).

[31] J.-P. Fouilloy and M. B. Sirieix, “History of infrared optronics in France,” Proc. SPIE, 2552 804 –814 (1995). http://dx.doi.org/10.1117/12.218281 PSISDG 0277-786X.

[32] M. J. Taylor et al., “Pulsed CO2 TEA laser rangefinder,” Appl. Opt., 17 885 –889 (1978). http://dx.doi.org/10.1364/AO.17.000885 APOPAI 0003-6935.

[33] H. Karning, J. F. Ruger and M. Weispfenning, “Concept and design of a multiple-function laser (MFL),” Proc. SPIE, 3436 433 –438 (1998). http://dx.doi.org/10.1117/12.328040 PSISDG 0277-786X.

[34] D. E. Smith et al., “Initial observations from the lunar orbiter laser altimeter (LOLA),” Geophys. Res. Lett., 37 L18204 (2010). http://dx.doi.org/10.1029/2010GL043751 GPRLAJ 0094-8276

[35] D. Inoue et al., “Highly sensitive LIDAR with a thumb-sized sensor-head built using an optical fiber preamplifier,” Proc. SPIE, 8731 87310Y (2013). http://dx.doi.org/10.1117/12.2016451 PSISDG 0277-786X

[36] T. Wilkerson et al., “VisibleWindTM: a rapid-response system for high-resolution wind profiling,” Proc. SPIE, 7460 746009 (2009). http://dx.doi.org/10.1117/12.826368 PSISDG 0277-786X

[37] Z. Liu et al., “Low-altitude atmospheric wind measurement from the combined Mie and Rayleigh backscattering by Doppler lidar with an iodine filter,” Appl. Opt., 41 7079 –7086 (2002). http://dx.doi.org/10.1364/AO.41.007079 APOPAI 0003-6935

[38] X. Dou et al., “Mobile Rayleigh Doppler lidar for wind and temperature measurements in the stratosphere and lower mesosphere,” Opt. Express, 22 A1203 –A1221 (2014). http://dx.doi.org/10.1364/OE.22.0A1203 OPEXFF 1094-4087

[39] C. L. Korb et al., “Theory of the double-edge technique for Doppler lidar wind measurement,” Appl. Opt., 37 3097 –3104 (1998). http://dx.doi.org/10.1364/AO.37.003097 APOPAI 0003-6935

[40] P. Lutzmann et al., “Laser vibration sensing: overview and applications,” Proc. SPIE, 8186 818602 (2011). http://dx.doi.org/10.1117/12.903671 PSISDG 0277-786X

[41] K. I. Schultz et al., “Satellite vibration measurements with an autodyne CO2 laser radar,” Appl. Opt., 33 2349 –2355 (1994). http://dx.doi.org/10.1364/AO.33.002349 APOPAI 0003-6935

[42] F. Hanson and M. Lasher, “Coherent laser radar at 3.6 μm,” Appl. Opt., 41 7689 –7693 (2002). http://dx.doi.org/10.1364/AO.41.007689 APOPAI 0003-6935

[43] S. W. Henderson et al., “Wind Lidar,” Laser Remote Sensing, 469 –722 CRC Taylor & Francis, Boca Raton, Florida (2005).

[44] J. M. Vaughan et al., “Coherent laser radar in Europe,” Proc. IEEE, 84 (2), 205 –226 (1996). http://dx.doi.org/10.1109/5.482229 IEEPAD 0018-9219

[45] Optical and Laser Radar Remote Sensing, 318 –381 Springer, Berlin, Heidelberg (1983).

[46] R. M. Huffaker, A. V. Jelalian and J. A. L. Thompson, “Laser-Doppler system for detection of aircraft trailing vortices,” Proc. IEEE, 58 322 –326 (1970). http://dx.doi.org/10.1109/PROC.1970.7636 IEEPAD 0018-9219

[47] T. Sakimura et al., “1.5 - μm high-gain and high-power laser amplifier using a Er, Yb:glass planar waveguide for coherent Doppler lidar,” in Proc. CLEO, 114 (2012).

[48] S. Kameyama et al., “Development of wind sensing coherent Doppler lidar at Mitsubishi Electric Corporation from late 1990s to 2013,” in Abstracts Int. Coherent Laser Radar Conf., (2013).

[49] N. Martin, R. Ganini and X. Chazelle, “CLARA-A Franco-British development of airborne laser radar,” in Proc. 7th Conf. on Coherent Laser Radar, Applications & Technology, (1993).

[50] B. Stephan and P. Metivier, “Flight evaluation trials of a heterodyne CO2 laser radar,” Proc. SPIE, 0806 9 (1987). http://dx.doi.org/10.1117/12.941404 PSISDG 0277-786X

[51] R. D. Callan et al., “Active airborne line scan experiment,” Proc. SPIE, 2272 183 –191 (1994). http://dx.doi.org/10.1117/12.191914 PSISDG 0277-786X

[52] D. Pierrottet et al., “Flight test performance of a high precision navigation Doppler lidar,” Proc. SPIE, 7323 732311 (2009). http://dx.doi.org/10.1117/12.821902 PSISDG 0277-786X

[53] G. Fiocco and L. O. Smullin, “Detection of scattering layers in the upper atmosphere (60–140 km) by optical radar,” Nature, 199 1275 –1276 (1963). http://dx.doi.org/10.1038/1991275a0

[54] R. T. H. Collis, F. G. Fernald and M. G. H. Ligda, “Laser radar echoes from the clear atmosphere,” Nature, 203 508 –508 (1964). http://dx.doi.org/10.1038/203508a0

[55] R. M. Schotland, “The determination of the vertical profile of atmospheric gases by means of a ground based optical radar,” in Proc. Third Symp. on Remote Sensing of Environment (1964), (1965).

[56] H. Inaba et al., “Fundamental study of operational performance of a laser radar system employing A-scope representation,” Electron. Commun. Jpn., 51-B 36 –52 (1968).

[57] Y. F. Arshinov, S. M. Bobrovnikov and S. V. Sapozhnikov, “On the technique of lidar measurement of the atmosphere temperature by signals ratio of the pure rotational spectra of N2 and O2,” Zhurnal Prikladnoy Spektroskopii, 32 (4), 725 –731 (1980).

[58] V. E. Zuev, Y. S. Makushkin and V. N. Matrichev, “Laser sensing of the humidity profile of the atmosphere,” Doklady AN SSSR, 257 (6), 1338 –1342 (1981).

[59] Weapons and Technologies in Russia. XXI Century, 720 Oruzhie i Tekhnologii, Moscow (2005).

[60] H. Hu and J. Qiu, “An overview of lidar study in China,” Rev. Laser Eng., 23 (2), 85 –88 (1994). http://dx.doi.org/10.2184/lsj.23.171 REKEDA 0387-0200

[61] S. Svanberg, Atomic and Molecular Spectroscopy: Basic Aspects and Applications, Springer, Berlin (2004).

[62] Laser Monitoring of the Atmosphere, Springer, Berlin (1976).

[63] V. I. Tatarskiy, Wave Propagation in Turbulent Atmosphere (in Russian), 548 Nauka, Moscow (1967).

[64] V. E. Zuev, Propagation of Laser Radiation in Atmosphere (in Russian), 287 Radio i Sviaz, Moscow (1981).

[65] C. R. Philbrick et al., "Optical remote sensing techniques to characterize the properties of atmospheric aerosols," Proc. SPIE, 7684 76840J (2010). http://dx.doi.org/10.1117/12.850453 PSISDG 0277-786X

[66] "Dynamic 3D imaging," in Proc. of the DAGM Workshop in Jena, 177 (2009).

[67] C. Grönwall et al., "An approach to target detection in forested scenes," Proc. SPIE, 6950 69500S (2008). http://dx.doi.org/10.1117/12.777042 PSISDG 0277-786X

[68] M. Koutsoupidou, I.S. Karanasiou, N. Uzunoglu, "Rectangular patch antenna on split-ring resonators substrate for THz brain imaging: modeling and testing", 13th IEEE Int. Conf. Bioinforma. Bioeng., IEEE (2013), pp. 1-4, 10.1109/BIBE.2013.6701595

[69] A. Sharma, V.K. Dwivedi, G. Singh, "THz rectangular microstrip patch antenna on multilayered substrate for advance wireless communication systems", Piers 2009 Beijing Progess Electromagn. Res. Symp. Proc. I Ii. (2009), pp. 627-631

[70] Radioastronomy - frequencies list, (2003) (n.d.). http://www.astrosurf.com/luxorion/radioastro-frequencieslist.htm.

[71] A. Sharma, G. Singh, "Rectangular microstirp patch antenna design at THz frequency for short distance wireless communication systems", J. Infrared, Millimeter Terahertz Waves, 30 (2008), p. 1, 10.1007/s10762-008-9416-z

[72] V. Molebny, P. F. McManamon, O. Steinvall, T. Kobayashi, and W. Chen, "Laser radar: historical prospective—from the East to the West," https://doi.org/10.1117/1.OE.56.3.031220, vol. 56, no. 3, p. 031220, Dec. 2016, doi: 10.1117/1.OE.56.3.031220.

[73] G. R. Koirala and A. Chhetry, "MXenes and their composites for flexible electronics," MXenes and their Composites: Synthesis, Properties and Potential Applications, pp. 423–447, Jan. 2021, doi: 10.1016/B978-0-12-823361-0.00022-8.

[74] M. Khulbe, M. R. Tripathy, H. Parthasarthy, and J. Dhondhiyal, "Dual Band THz Antenna Using T Structures and Effect of Substrate Volume on Antenna Parameters,"

Proceedings - 2016 8th International Conference on Computational Intelligence and Communication Networks, CICN 2016, pp. 191–195, Oct. 2017, doi: 10.1109/CICN.2016.43.

[75] M. S. Rabbani and H. Ghafouri-Shiraz, “Liquid Crystalline Polymer Substrate-Based THz Microstrip Antenna Arrays for Medical Applications,” IEEE Antennas Wirel Propag Lett, vol. 16, pp. 1533–1536, 2017, doi: 10.1109/LAWP.2017.2647825.

[76] M. A. Chung and B. R. Chuang, “Design a Broadband U-Shaped Microstrip Patch Antenna on Silicon-Based Technology for 6G Terahertz (THz) Future Cellular Communication Applications,” IEMECON 2021 - 10th International Conference on Internet of Everything, Microwave Engineering, Communication and Networks, 2021, doi: 10.1109/IEMECON53809.2021.9689167.

[77] A. S. Dhillon, D. Mittal, and E. Sidhu, “THz rectangular microstrip patch antenna employing polyimide substrate for video rate imaging and homeland defence applications,” Optik (Stuttg), vol. 144, pp. 634–641, Sep. 2017, doi: 10.1016/J.IJLEO.2017.07.018.

[78] S. Sen Yao, Y. J. Cheng, Y. F. Wu, and H. N. Yang, “THz 2-D Frequency Scanning Planar Integrated Array Antenna with Improved Efficiency,” IEEE Antennas Wirel Propag Lett, vol. 20, no. 6, pp. 983–987, Jun. 2021, doi: 10.1109/LAWP.2021.3068773.

[79] L. Guo, Hongfu Meng, Lei Zhang, and Jun Ge, “Design of MEMS on-chip helical antenna for THz application,” pp. 1–4, Oct. 2016, doi: 10.1109/IMWS-AMP.2016.7588385.

[80] IRMMW-THz 2018 : 2018 43rd International Conference on Infrared, Millimeter and Terahertz Waves : conference guide : Nagoya Congress Center, Nagoya, Japan.